KWAME NKRUMAH UNIVERSITY OF SCIENCE AND
TECHNOLOGY, KUMASI

COLLEGE OF SCIENCE

DEPARTMENT OF MATHEMATICS

DISCONTINUOUS GALERKIN ISOGEOMETRIC ANALYSIS FOR THE BIHARMONIC PROBLEM

A THESIS SUBMITTED TO THE DEPARTMENT OF MATHEMATICS THROUGH THE NATIONAL INSTITUTE FOR MATHEMATICAL SCIENCES IN PARTIAL FULFILLMENT OF THE REQUIREMENTS FOR THE AWARD
OF
MASTER OF PHILOSOPHY DEGREE
(SCIENTIFIC COMPUTING & INDUSTRIAL MODELING)

BY
JOSHUA AMEVIALOR
MARCH, 2017

Declaration

I hereby declare that, this thesis is the result of my own original research and that no part of it has been submitted to any institution or organization anywhere for the award of a degree. All inclusion for the work of others has been dully acknowledged.

Joshua, Amevialor	.....	.....
Student (PG3325114)	Signature	Date

Certified by:

Dr. P. Amoako-Yirenkyi	.....	.....
Member, Supervisory Committee	Signature	Date
Prof. I. K. Dontwi	.....	.....
Member, Supervisory Committee	Signature	Date
Dr. S. E. Moore	.....	.....
Member, Supervisory Committee	Signature	Date
Dr. R. K. Avuglah	.....	.....
Head of Department	Signature	Date

Abstract

The biharmonic problem is an example of a fourth order elliptic partial differential equation (PDE). Fourth order elliptic PDEs are of interest in a wide range of applications including linear elasticity, fluid dynamics, biology, pattern formation, solid mechanics and electromagnetics. Isogeometric Analysis (IgA), proposed in 2005 by T. Hughes, J. Cottrell and Y. Bazilevs, is a numerical method that uses the same class of basis functions for both representing the geometry of the computational domain and approximating the solution of problems governed by PDEs. Isogeometric analysis is based on B-spline and Non-Uniform Rational B-Spline (NURBS), which are the main tools used in most engineering design packages. The use of NURBS makes it possible to construct basis functions with higher smoothness with relative ease due to their special properties, thus making it a suitable choice for working with higher order PDEs. Discontinuous Galerkin Isogeometric Analysis (dG-IgA) provides a means for coupling multiple patches that occur in most practical applications. As is usually the case, the computational domains in many engineering applications cannot be represented by a single NURBS geometry mapping and are thus decomposed into several sub-domains or patches. In this thesis, a dG-IgA scheme is proposed for the biharmonic problem, and *a-priori* error estimates are obtained for geometrically matching sub-domains with matching meshes. It is concluded that, dG-IgA is a feasible option for solving higher order PDEs. From the theoretical results obtained, the proposed dG-IgA scheme converges optimally in the dG-norm.

Acknowledgements

I would like to take this opportunity to thank my supervisors, S. E. Moore, P. Amoako-Yirenkyi and I. K. Dontwi for their guidance, inputs and discussions that culminated in the successful completion of this thesis.

I am grateful to the National Institute for Mathematical Sciences, Ghana (NIMS-Ghana), for the "Scientific Computing and Industrial Modeling" program and the corresponding scholarship, and providing the environment to make this work possible.

Finally, special thanks to my family and friends for their support, encouragement and prayers.

Joshua Amevialor

Kumasi, February 2017

Dedication

This thesis is dedicated to my father, Paul Amevialor, my mother, Christina Tetteh, and my siblings, Bliss Selasi and Daniel Delali.

Contents

List of Tables

List of Figures

Chapter 1
Introduction

1.1 Background

Prior to the advent of Isogeometric Analysis (IgA), it was necessary to convert data between Computer Aided Design (CAD) and Finite Element Analysis (FEA) packages to analyze new designs during development. This process is a daunting and time intensive task, since the computational geometric approach for each was different, Hughes et al. (2005). According to some engineers, about 80% of the time used for analysis is spent on the conversion and mesh generation. Isogeometric Analysis however, is premised on the use of complex NURBS geometry (which is the basis of most CAD packages) in the FEA application directly, thereby making it feasible for models to be designed, tested and adjusted at once using a common data set, Hughes et al. (2005), Cottrell et al. (2009).

According to Hughes et al. (2005), Cottrell et al. (2006), Bazilevs et al. (2006), the primary objectives for IgA are the following.

1. To provide a more accurate representation of complex geometries and exact representations of shapes like circles, spheres, ellipsoids etc. for analysis.

2. To maintain geometric exactness at the coarsest level of discretization.

3. To eliminate the need to communicate with the CAD description of geometry during mesh refinements.

4. To provide mesh refinement strategies that make the preceding objective possible and provide analogues of h-refinement and p-refinement.

These objectives have been achieved and the k-refinement strategy was also introduced. The main ideas and procedures of IgA are presented in Hughes et al. (2005), Cottrell et al. (2006), Cottrell et al. (2009). The authors also present compelling numerical results. Bazilevs et al. (2006) focused more on the challenges in obtaining the appropriate approximation estimates for an analysis framework based on NURBS.

In Hughes et al. (2005), the authors provide estimates of the FEA industry and the CAD industry. They conclude that it is more industrially relevant to attack the problem of the unification of CAD and FEA from a more CAD based direction. NURBS, being the dominant tool in most CAD packages, was chosen as the basis for analysis in IgA. NURBS have also been shown to have some properties that make them suitable for analysis. Hughes et al. (2005) enumerates some of the items and features of an analysis framework based on NURBS.

Some of the applications of IgA are listed in Nguyen et al. (2015), and includes the analysis and discretization of contact problems. Where the use of conventional geometry discretization, require very fine meshes in order to minimize jumps and oscillations in traction responses when dealing with faceted surfaces. It has been shown that this can be resolved by using NURBS, since smooth contact surfaces can then be obtained, leading to more physically accurate contact stresses.

It is observable from available literature that there has been a lot of work done on building the framework for working with and analyzing second and first order PDEs. Even restricted to just finite element schemes, the list is nigh in-exhaustive. Work on higher order PDEs are relatively fewer, which in part is due to the nature and complexity of the finite elements needed to work with them. The issue of high continuity approximation spaces however, could be solved with the introduction of IgA. From available literature, the Isogeometric paradigm has been applied to almost all benchmark second order partial differential equations and some higher order partial differential equations using the standard Galerkin approach, see e.g. Auricchio et al. (2007); Vuong et al. (2010); Tagliabue et al. (2014); Bartezzaghi et al. (2015).

Handling multiple patches is an important part of IgA, since the computational domains in many engineering applications are represented by multiple NURBS patches. In Cottrell et al. (2009), a method for gluing multiple patches by introducing a set of constraint equations is described. There is on-going research into finding alternate means of coupling patches in IgA.

1.2 Motivation

Progress in the numerical computing community is fuelled by the need and desire to develop and implement faster, more efficient and mathematically sound algorithms and procedures for solving pertinent problems.

Isogeometric Analysis has shown a number of advantages over classical FEA, see e.g. Nguyen et al. (2015). As mentioned earlier, handling multiple patches is a critical part of the development of IgA. With more options as to how to couple patches, it would be possible to investigate and determine which approaches are convenient or

better for various situations. This would allow for more flexibility and could increase the scope of the industrial relevance and applications of IgA.

In Nguyen et al. (2014), a Nitsche method is proposed as an alternative for coupling NURBS patches in IgA. Discontinuous Galerkin Isogeometric Analysis (dG-IgA) has also been introduced and shown to provide a means for coupling multiple patches. There have been investigations into using dG-IgA and this has been done for most second order PDEs, see e.g. Brunero (2012); Langer and Toulopoulos (2014); Langer et al. (2014); Zhang et al. (2015); Langer and Moore (2016). It has been observed that the discontinuous Galerkin approach combines well with multi-patch and complex geometries. However, from the literature observed, dG-IgA has yet to be studied in the context of high order PDEs.

1.3 Problem Statement

There are a number of industrially relevant high order PDEs. Fourth order elliptic problems for instance, come up in linear elasticity, fluid dynamics, and solid mechanics among others. High order PDEs have been studied in the context of IgA using the standard Galerkin approach, see e.g. Gomez et al. (2009), Tagliabue et al. (2014), and Bartezzaghi et al. (2015).

Discontinuous Galerkin Isogeometric Analysis, among other things, offers a means of coupling multiple patches. This has been analyzed and tested for several second order PDEs with compelling results as to the feasibility of the approach. To extend the applicable scope of the method, there is a need to analyze the method in the context of higher order PDEs.

This thesis aims to apply dG-IgA to the biharmonic problem. Using techniques from Engel et al. (2002), Mozolevski and Süli (2003), Pietro and Ern (2012), Hughes et al. (2005) and Bazilevs et al. (2006), *a-priori* error estimates are presented.

1.4 Objective

The objectives of this thesis are:

1. To derive the standard Galerkin IgA approximation for the general biharmonic problem and the corresponding *a-priori* error estimates;

2. To derive an interior penalty variational formulation for the Dirichlet version of the biharmonic problem, and obtain a discontinuous Galerkin Isogeometric Analysis (dG-IgA) approximation;

3. To show the existence, uniqueness and stability of the solution to the model problem;

4. To obtain *a-priori* error estimates for the proposed formulation.

1.5 Outline of the Methodology

First, the standard Galerkin IgA formulation for the general biharmonic problem is derived. Existence and uniqueness are shown by invoking the Lax-Milgram Lemma, and showing that the necessary prerequisites are satisfied. From the results presented in Bazilevs et al. (2006), Tagliabue et al. (2014), *a-priori* error estimates are presented for the single patch problem with h-refined meshes.

Next, following the approach in Brunero (2012), Langer and Toulopoulos (2014), Langer et al. (2014), an interior penalty variational formulation for the Dirichlet version of the biharmonic problem is derived. A dG-IgA scheme is obtained from

this variational formulation. Consistency is shown using standard arguments for discontinuous Galerkin methods, see Riviére (2008), Pietro and Ern (2012). Using arguments similar to those used in Brunero (2012), Mozolevski and Süli (2003), discrete coercivity and boundedness of the bilinear form are shown.

Some pertinent auxiliary results from Bazilevs et al. (2006), Tagliabue et al. (2014) and Moore (2017) are presented, and estimates for the interface integrals are derived. Subsequently, *a-priori* error estimates for multiple geometrically matching patches with matching meshes are presented.

1.6 Justification of the Study

The work presented in this thesis provides a starting point for using dG-IgA for high-order PDEs like the Cahn-Hilliard equation, the Euler-Bernoulli beam equation etc. which are industrially relevant.

The combination of the high continuity offered by IgA and the flexibility offered by the discontinuous Galerkin approach is worth investigating. In Auricchio et al. (2007), the authors recommended the discontinuous Galerkin Isogeometric analysis formulation as a viable extension to their work.

Due to the tensor product nature of NURBS basis functions, refinements tend to be global. This has been noted as one of the shortcomings of NURBS-based IgA (Nguyen et al., 2015). Aside from providing a means for coupling NURBS patches, using the discontinuous Galerkin approach makes it possible to carry out local refinements.

1.7 Organization of Chapters

In chapter 1, IgA is briefly presented and its primary objectives are recalled. Some of the advantages of IgA are mentioned as well as some of the challenges encountered in its development. The works that motivated this thesis and reasons why dG-IgA is worth investigating for higher order PDEs are also discussed.

In chapter 2, a review of available literature on IgA is presented. Though some non-Galerkin-based Isogeometric methods have been proposed recently, this review is restricted to Galerkin based IgA methods.

In chapter 3, function spaces and some operations pertinent to the analysis of PDEs are recalled. The basic features of Isogeometric Analysis are also recalled in more detail; specifically the basis used (B-spline and NURBS) and the tools necessary for their development, some of their properties, as well as the available refinement strategies. Subsequently, a discussion on the viability of NURBS as a basis for analysis is presented. Next, the biharmonic problem is introduced and the variational formulation for the problem is derived. The existence, uniqueness and stability of the solution to the model problem is shown. The Galerkin equations for the biharmonic problem, on finite dimensional NURBS spaces (single patch) are obtained. *A-priori* error estimates are presented for the derived scheme for h-refined meshes.

In chapter 4, an interior penalty Galerkin scheme for the biharmonic problem is derived and consistency is shown. The existence and uniqueness of the solution to the model problem is shown. Next, approximation estimates for NURBS are presented, and *a-priori* error estimates are obtained for the dG-IgA scheme derived for the biharmonic problem on h-refined meshes.

Finally, conclusions and recommendations for further research are presented in chapter 5.

Chapter 2

Literature Review

2.1 Introduction

In this chapter, a brief review of literature on IgA is presented. Most methods and procedures in IgA are similar to those used in classical FEA, as the methods have just been adapted to use a different class of basis. Literature on IgA thus mostly involves the adaptation of the various methods in classical FEA, to varying problems using the Isogeometric paradigm. To be consistent with the rest of the work in this thesis, this review is restricted to work on NURBS-based IgA using the Galerkin approach.

2.2 Literature Review

Finite element methods were introduced in the 1950s as a means to obtain approximate solutions to PDEs. Finite element methods are employed in FEA packages, and have become a major part of engineering analysis. Solution of PDEs by the finite element method roughly consists of a variational formulation of the problem, and trial and test function spaces defined by their respective basis functions. These

basis functions are defined by a non-overlapping decomposition of the problem domain into simple shapes, dubbed "finite elements", and are usually represented by piece-wise polynomial functions. Over the years, finite element methods have been extensively studied and applied to a wide range of problems, with numerous books and articles to that effect, see e.g. Hughes (2000); Ciarlet (2002); Brenner and Scott (2008); Nečas (2012).

Discontinuous Galerkin methods are finite element methods which were first introduced for hyperbolic problems, and have also been applied to elliptic and parabolic problems, see Riviére (2008) and Pietro and Ern (2012). Discontinuous Galerkin methods allow for discontinuities in the trial and test spaces, making it possible to localize test functions to single mesh elements and introducing numerical fluxes at interfaces. Interest in discontinuous Galerkin methods has increased over the years, and they have seen more mathematically rigorous development. In Arnold et al. (2002), a unified discontinuous Galerkin framework was presented for second order elliptic problems. Discontinuous Galerkin methods have also been considered for higher order problems, see e.g. Engel et al. (2002) and Süli and Mozolevski (2007). Computer Aided Design packages are typically used by engineers for designing. This ranges from designing new types of aircraft or underground works to simply creating digital representations of geometry (Beer, 2015). Over the years, the CAD industry has seen a lot of innovation, with the introduction of various CAD representations. Hughes et al. (2005) gives an outline of the evolution of CAD representations and FEA basis function over the years.

Isogeometric Analysis presents an alternative to classical FEA, and was necessitated by the bottleneck in computational speed in engineering analysis due to the lack of a direct link between CAD and FEA. In Hughes et al. (2005), the authors showed that

NURBS basis could be used for both geometric representation and analysis, thereby reducing the time spent in the mesh generation phase for analysis of design models created using CAD. Analogues of the refinement strategies in FEA (h-refinement and p-refinement) were also presented together with a higher level refinement strategy (k-refinement). The procedures for refinement were designed such that the geometry or its parametrization remained unchanged, eliminating the need to communicate with the CAD description of geometry during mesh refinements.

In Table 2.1 the differences between IgA and classical FEA have been summarized, see Hughes et al. (2005).

Table 2.1: Comparison of Finite Element Analysis and NURBS-based Isogeometric Analysis

Finite Element Analysis	**Isogeometric Analysis**
Nodal points	Control points
Nodal variables	Control variables
Mesh	Knots
Basis interpolates-	Basis does not interpolate-
-nodal points and variables	-control points and variables
Approximate geometry	Exact geometry
Polynomial basis	NURBS basis
Gibbs phenomena	Variation diminishing
Sub-domains	Patches
Compact support	
Partition on unity	
Isoparametric concept	
Affine covariance	
Patch tests satisfied	

Isogeometric Analysis was used to solve a number of sample problems from linear solid and structural mechanics and fluid mechanics. For the infinite plate modeled by a quarter plate with a circular hole, the authors obtained optimal convergence rates in the L^2 norm. Optimal convergence rates were obtained in the energy norm for a solid circular cylinder subjected to internal pressure loading. Other sample problems

considered included the Scordelis-Lo roof, pinched hemisphere, pinched cylinder and advection-diffusion problems in fluid dynamics.

The authors identified several areas of IgA that required more research. These included finding a robust strategy for numerical quadrature under various conditions for NURBS, developing a mathematical theory of convergence and error analysis, applying IgA to contact problems and other problems of engineering interest. This list is by no means exhaustive, and these areas are still being investigated.

In the monograph Cottrell et al. (2009), it was noted that, in order to obtain *a-priori* error estimates for NURBS-based IgA analogous to those available for classical finite element methods, there were several challenges. The first being that the approximation properties of the rational basis were more difficult to determine than those of a standard polynomial basis. In particular, the weights associated with NURBS were determined by the geometry and could not be adjusted to improve results when attempting to approximate a field over that geometry.

The second difficulty was attributed to the relatively large support of the spline functions (that is, $p+1$ "elements", p being the polynomial degree of the spline functions). Standard interpolation estimates are usually obtained by finding best fits within each element and then summing these results over all elements in the mesh to obtain a global approximation estimate. The larger supports of the spline functions make obtaining approximation estimates a non-trivial task, since it is virtually impossible to determine optimal values for the control variables by considering each element individually. The issue was noted to be further complicated by the possible occurrence of differing levels of continuity. This meant that there was the possibility of having differing sizes of supports of functions throughout the domain.

In IgA, the geometry of the mapping between a d-cube in the parametric space ($d = 1, 2, 3$) and its image in the physical space requires the introduction of concepts and spaces not utilized in standard FEA. In Bazilevs et al. (2006), it was noted that, for interpolants of sufficiently high continuity, it was not feasible to stay in a single element and invoke a standard Bramble-Hilbert estimate. To handle the problem of the large support of the NURBS basis, and to develop the framework for the approximation properties for NURBS, the authors introduced a non-standard Hilbert space which they called "bent" Sobolev spaces. These spaces incorporated the notion of "support extensions". The authors went ahead to present inequalities and estimates necessary to obtain error estimates for h-refined meshes. The sample problems considered include the classical linear elasticity problem, the advection diffusion problem and the driven cavity problem.

According to Auricchio et al. (2010), the use of high-degree basis functions, as in k-refinement, raises the issue of efficient implementation, with respect to the numerical quadrature rules adopted when assembling the system of equations. Specifically, while element-wise Gauss quadrature is known to be optimal in the finite element context, it has been observed to be sub-optimal when k-refined Isogeometric discretization of Galerkin type are considered. In response, in Hughes et al. (2010), the authors derive and present a number of more efficient specialized rules for IgA.

In Nguyen et al. (2015), the authors present an overview of IgA, providing some applications of IgA and also give quite an extensive list of the research that has been carried out under the IgA paradigm. They point out areas in which IgA has exhibited advantages over the classical finite element methods. These areas include contact problems, optimization problems and shell and plate problems. They also

note that, the smoothness of NURBS basis functions makes them attractive for analysis of fluids and for fluid-structure interaction problems. Due to the relative ease with which high order continuous basis functions can be constructed in IgA, it has subsequently been used with a substantial amount of success in solving PDEs that involve fourth order (or higher) derivatives of the field variable such as the Cahn-Hilliard equation. The authors also make mention of some of the shortcomings of using NURBS. These include the inability of NURBS to produce watertight geometries, which can lead to complications in mesh generation. Also, due to the tensor product nature of NURBS, refinement operations tend to be global, leading to inefficient error estimation and trouble with adaptivity algorithms. The authors also discuss some aspects of computer implementations for IgA.

Multiple patch NURBS are used to represent objects with complex geometries. In Cottrell et al. (2009), multiple patches were glued together using exact constraint equations, under the restriction that the coarsest meshes had the same parametrization. A Nitsche method for coupling two and three dimensional NURBS patches was presented in Nguyen et al. (2014), and provides an alternative means of coupling patches. Nitsche's method was originally proposed and is usually used to weakly enforce Dirichlet boundary conditions. The authors proposed a method that used Nitsche's approach to couple patches, under the assumption that, some other method is used to enforce the essential boundary conditions other than the Nitsche method. The method was applied to the Timoshenko beam problem and the Cantilever beam problem among others, and convergence analysis were presented for the Timoshenko beam problem.

In Brunero (2012), a dG-IgA scheme was proposed for the scalar diffusion problem. This is arguable the first time IgA was rigorously combined with discontinuous

Galerkin methods, though the idea had been recommended in Auricchio et al. (2007). A number of useful inequalities for dG-IgA were presented. An interior penalty variational formulation was obtained for the diffusion problem and existence and uniqueness of the solution to the model problem were shown via the Lax-Milgram lemma by showing coercivity and boundedness of the bilinear form. Numerical analysis were performed on the dG-IgA scheme for matching meshes. No numerical results were presented for the proposed scheme, however, the author outlines some steps for the implementation of the scheme.

In Langer and Toulopoulos (2014), the approximation properties of dG-IgA methods were studied in the context of second order elliptic problems with discontinuous coefficients. *A-priori* error estimates are presented for usual regularity and low regularity assumptions on the exact solution. Numerical results were presented that showed optimal convergence rates in the dG-norm.

Discontinuous Galerkin Isogeometric Analysis schemes are further studied in Langer et al. (2014) and Langer and Moore (2016) for second order heterogeneous elliptic problems in 2 and 3 dimensions and open and closed surfaces. Theoretical and numerical results are presented for patches with matching and non-matching meshes. The authors also introduced graded mesh techniques in dG-IgA for problems with singularities.

On software implementation, it is noteworthy that a number of softwares have been developed that implement the IgA concept, mostly as extensions in existing FEA programs. According to Vázquez (2016), in the last few years, a number of new IgA softwares have been released:

1. GeoPDEs, and at least one more package written in MATLAB, focused on computational solid mechanics.

2. Igatools, which is a C++ library providing dimension independent implementation of IgA.

3. G+Smo, another C++ library for IgA which also includes implementations for hierarchical splines, Jüttler et al. (2014).

4. PetIGA, a C implementation of Isogeometric methods based on PETSc, and according to Vázquez (2016), has been recently extended to include the curl- and div-conforming spline discretization.

Chapter 3

Methodology

3.1 Introduction

In this chapter, function spaces and some operations relevant to the analysis of PDEs are recalled. Next, B-splines and NURBS and their use in IgA is presented. Finally, the biharmonic problem is presented and the variational formulation of the problem is derived. Uniqueness and existence of the solution to the model problem are shown and *a-priori* error estimates are presented for the single patch case.

3.2 Preliminaries

In this section, some pertinent function spaces are introduced. The definitions in this section are mostly taken from Riviére (2008), Adams and Fournier (2003) and Lions and Magenes (1972).

Let Ω be an open bounded Lipschitz domain in $\mathbb{R}^d$, $d = 1, 2, 3$, with Lipschitz continuous boundary $\Gamma = \partial\Omega$. The symbol, ∇, denotes the gradient of a smooth function $u : \mathbb{R}^d \to \mathbb{R}$, i.e., $\nabla u = \left(\frac{\partial u}{\partial x_1}, \cdots, \frac{\partial u}{\partial x_d}\right)$. Let $C_0^1(\Omega; \mathbb{R}^d)$ denote the space of vector-

valued functions $\boldsymbol{\varphi} = (\varphi_1, \ldots, \varphi_d)$ whose component functions φ_i; $i = 1, \ldots, d$, are continuously differentiable and compactly supported on Ω. The divergence of $\boldsymbol{\varphi}$ is given by

$$div\boldsymbol{\varphi} = \nabla \cdot \boldsymbol{\varphi} = \sum_{i=1}^{d} \frac{\partial \varphi_i}{\partial x_i}\,.$$

Definition 3.2.1. The support of a continuous function u defined on $\mathbb{R}^d$ is the closure of the set of points at which the function is not equal to zero. If it is bounded and included in the interior of the domain Ω, then u is said to have compact support in Ω.

Given a multi-index $\boldsymbol{\alpha} = (\alpha_1, \alpha_2, \ldots, \alpha_d) \in \mathbb{N}^d$, a locally integrable function w is said to be the $\boldsymbol{\alpha}$th *weak partial derivative* of a locally integrable function u if

$$\int_\Omega u(\mathbf{x}) D^{\boldsymbol{\alpha}} v(\mathbf{x}) \mathrm{d}\Omega = (-1)^{|\boldsymbol{\alpha}|} \int_\Omega w(\mathbf{x}) v(\mathbf{x}) \mathrm{d}\Omega \quad \forall v \in C_0^\infty(\Omega), \tag{3.1}$$

where $C_0^\infty(\Omega)$ is the space of all infinitely differentiable functions with compact support, and the partial derivative with respect to $\boldsymbol{\alpha}$ is given by

$$D^{\boldsymbol{\alpha}} v = \frac{\partial^{|\boldsymbol{\alpha}|} v}{\partial x_1^{\alpha_1} \cdots \partial x_d^{\alpha_d}},$$

with $|\boldsymbol{\alpha}| = \sum_{i=1}^{d} \alpha_i$. Then, w can be denoted by $w = D^{\boldsymbol{\alpha}} u$.

Definition 3.2.2 (L^p Spaces)**.** Let Ω be a domain in $\mathbb{R}^n$ and let p be a positive real number. Denote by $L^p(\Omega)$ the class of all measurable functions u defined on Ω for which

$$\int_\Omega |u(\mathbf{x})|^p \mathrm{d}\Omega < \infty\,.$$

The norm on $L^p(\Omega)$ is given by

$$\|u\|_{L^p(\Omega)} = \begin{cases} \left(\int_\Omega |u(\mathbf{x})|^p \mathrm{d}\Omega\right)^{\frac{1}{p}}, & p \in [1, \infty), \\ ess\sup\{|u(\mathbf{x})| : \mathbf{x} \in \Omega\}, & p = \infty\,. \end{cases}$$

As an example, for $p = 2$, there is $L^2(\Omega)$, the space of Lebesgue measurable, square-integrable functions over Ω

$$L^2(\Omega) := \{u \text{ measurable } : \int_\Omega |u(\mathbf{x})|^2 \mathrm{d}\Omega < \infty\}\,.$$

Remark 3.2.1. Sobolev spaces, generally, are Banach spaces of Lebesgue measurable functions with varying orders of weak derivatives, and are quite essential to the study of the theory of partial differential equations and related areas of mathematical analysis, see Adams and Fournier (2003) for more detail.

Definition 3.2.3 (Sobolev Spaces)**.** For any positive integer m and $1 \leqslant p \leqslant \infty$, the Sobolev space $W^{m,p}(\Omega)$ is defined as

$$W^{m,p}(\Omega) := \{u \in L^p(\Omega) : \quad \forall 0 \leqslant |\boldsymbol{\alpha}| \leqslant m,\, D^{\boldsymbol{\alpha}} u \in L^p(\Omega)\}.$$

Definition 3.2.4 (The Sobolev Norms)**.** Define a functional $\|\cdot\|_{W^{m,p}}$, where m is a positive integer and $1 \leqslant p \leqslant \infty$, as follows:

$$\|u\|_{W^{m,p}} = \left(\sum_{0 \leqslant |\boldsymbol{\alpha}| \leqslant m} \|D^{\boldsymbol{\alpha}} u\|^p_{L^p(\Omega)}\right)^{\frac{1}{p}}, \quad p \in [1, \infty),$$

$$\|u\|_{W^{m,\infty}} = \max_{0 \leqslant |\boldsymbol{\alpha}| \leqslant m} \|D^{\boldsymbol{\alpha}} u\|_{L^\infty(\Omega)}.$$

Remark 3.2.2. Sobolev spaces of particular interest are those formed from L^2 spaces. With appropriate norms and inner products defined, these form Hilbert spaces, that is, complete inner product spaces.

Definition 3.2.5. Let s be an integer, then the Hilbert space $H^s(\Omega)$ is given by

$$H^s(\Omega) := \{u \in L^2(\Omega) : \quad \forall 0 \leqslant |\boldsymbol{\alpha}| \leqslant s,\, D^{\boldsymbol{\alpha}} u \in L^2(\Omega)\},$$

with the norm

$$\|u\|_{H^s(\Omega)} = \left(\sum_{0 \leqslant |\boldsymbol{\alpha}| \leqslant s} \|D^{\boldsymbol{\alpha}} u\|^2_{L^2(\Omega)} \right)^{\frac{1}{2}},$$

the seminorm

$$|u|_{H^s(\Omega)} = \|\nabla^s u\|_{L^2(\Omega)} = \left(\sum_{|\boldsymbol{\alpha}| = s} \|D^{\boldsymbol{\alpha}} u\|^2_{L^2(\Omega)} \right)^{\frac{1}{2}}.$$

and the inner product

$$(u, v)_{H^s(\Omega)} = \sum_{0 \leqslant |\boldsymbol{\alpha}| \leqslant s} (D^{\boldsymbol{\alpha}} u, D^{\boldsymbol{\alpha}} v)_{L^2(\Omega)}.$$

The $L^2(\Omega)$ space equipped with the norm

$$\|u\|_{L^2(\Omega)} = \left(\int_\Omega |u(\mathbf{x})|^2 \mathrm{d}\Omega \right)^{\frac{1}{2}},$$

and the inner product

$$(u, v)_{L^2(\Omega)} = \int_\Omega u(\mathbf{x}) v(\mathbf{x}) \mathrm{d}\Omega,$$

is a Hilbert space, and can be denoted by $H^0(\Omega)$.

Next, the relation between the Sobolev spaces and the r-times continuously differentiable functions is presented.

Theorem 3.2.1 (Sobolev's Embedding Theorem)**.** *For $\Omega \subset \mathbb{R}^d$, we have*

$$H^s(\Omega) \subset C^r(\Omega) \quad \text{if} \quad \frac{s - r}{d} > \frac{1}{2}. \tag{3.2}$$

Proof. See Riviére (2008); Adams and Fournier (2003). □

As an example for $r = 0$, we have the following conditions:

$$H^s(\Omega) \subset C^0(\Omega) \text{ if } \begin{cases} s > \frac{1}{2} \text{ for } d = 1, \\ s > 1 \text{ for } d = 2, \\ s > \frac{3}{2} \text{ for } d = 3. \end{cases}$$

Next, the trace theorem is recalled. This is the restriction of Sobolev spaces along the boundary.

Theorem 3.2.2 (Trace Theorem)**.** *Let Ω be a bounded domain with Lipschitz boundary Γ and outward normal vector $\mathbf{n}$. There exist trace operators $\gamma_0 : H^s(\Omega) \to H^{s-1/2}(\Gamma)$ for $s > \frac{1}{2}$ and $\gamma_1 : H^s(\Omega) \to H^{s-3/2}(\Gamma)$ for $s > \frac{3}{2}$ that are extensions of the boundary values and boundary normal derivatives, respectively. The operators γ_0, γ_1 are surjective. Furthermore, if $v \in C^1(\overline{\Omega})$, then*

$$\gamma_0 v = v|_\Gamma, \quad \gamma_1 v = \mathbf{n} \cdot \nabla v|_\Gamma. \tag{3.3}$$

Proof. See [Riviére (2008); Lions and Magenes (1972)]. □

For convenience, when dealing with function values and normal derivatives on boundaries, v and $\mathbf{n} \cdot \nabla v$ are written instead of the trace $\gamma_0 v$ and $\gamma_1 v$, respectively.

Let $\mathcal{T}_h := \{\Omega_i\}_{i=1}^N$, be a collection of sub-domains of a domain, Ω, such that

$$\overline{\Omega} = \bigcup_{i=1}^{N} \overline{\Omega}_i \,, \quad \text{with } \Omega_i \bigcap \Omega_j = \varnothing, \text{ if } i \neq j \,.$$

Then a broken Sobolev space, $H^s(\Omega, \mathcal{T}_h)$, is defined as

$$H^s(\Omega, \mathcal{T}_h) := \{u \in L^2(\Omega) : u|_{\Omega_i} \in H^s(\Omega_i), \quad \forall i = 1, \ldots, N\},$$

equipped with the norm

$$\|u\|_{H^s(\Omega, \mathcal{T}_h)} = \left(\sum_{i=1}^{N} \|u\|^2_{H^s(\Omega_i)} \right)^{\frac{1}{2}},$$

and the seminorm

$$|u|_{H^s(\Omega,\mathcal{T}_h)} = \left(\sum_{i=1}^{N} |u|^2_{H^s(\Omega_i)}\right)^{\frac{1}{2}}.$$

Broken Sobolev spaces are natural spaces for working with discontinuous Galerkin methods.

Next, the Young and Cauchy-Schwarz inequalities that will be used in several places are recalled.

Young's inequality is stated as follows

$$\forall \epsilon > 0, \quad \forall a, b \in \mathbb{R}, \quad ab \leqslant \frac{\epsilon}{2}a^2 + \frac{1}{2\epsilon}b^2. \tag{3.4}$$

The Cauchy-Schwarz inequality is given by

$$\left|\int_\Omega fg \mathrm{d}\Omega\right| \leqslant \left(\int_\Omega |f|^2 \mathrm{d}\Omega\right)^{\frac{1}{2}} \left(\int_\Omega |g|^2 \mathrm{d}\Omega\right)^{\frac{1}{2}}, \quad \forall f, g \in L^2(\Omega). \tag{3.5}$$

Lemma 3.2.3 (The Poincaré-Friedrichs' inequality)**.** *There exists a constant C_1, depending only on the domain Ω, such that*

$$\|v\|_{L^2(\Omega)} + \|\nabla v\|_{L^2(\Omega)} \leqslant C_1 \|\Delta v\|_{L^2(\Omega)}, \quad \forall v \in H^2_0(\Omega), \tag{3.6}$$

where $H^2_0(\Omega) := \{v \in H^2(\Omega) : v|_{\partial\Omega} = \mathbf{n} \cdot \nabla v|_{\partial\Omega} = 0\}$, $\mathbf{n}$ is the unit normal vector to $\partial\Omega$.

Proof. See Ciarlet (2002); Nečas (2012) □

Theorem 3.2.4 (Divergence Theorem)**.** *If Ω is a domain in $\mathbb{R}^2$ with smooth or piecewise smooth boundary and F is a vector field defined on $\overline{\Omega}$, then the divergence theorem states that*

$$\int_\Omega \nabla \cdot F \, d\Omega = \int_\Gamma (\mathbf{n} \cdot F) \, d\Gamma \tag{3.7}$$

where $\mathbf{n}$ is the outward pointing unit normal vector to Γ.

Green's first identity is given by

$$-\int_{\Omega} \varphi \Delta \omega \, \mathrm{d}\Omega = \int_{\Omega} \nabla \varphi \cdot \nabla \omega \, \mathrm{d}\Omega - \int_{\Gamma} \varphi (\mathbf{n} \cdot \nabla \omega) \, \mathrm{d}\Gamma, \tag{3.8}$$

and follows from the following product rule in multiple dimensions, given by

$$\nabla \cdot (\varphi \nabla \omega) = \nabla \varphi \cdot \nabla \omega + \varphi \Delta \omega \,, \tag{3.9}$$

and the divergence theorem.

3.3 B-splines and NURBS

In this section, the construction of B-splines and NURBS is recalled. Most of the definitions presented and the concepts illustrated are taken from the monograph, Cottrell et al. (2009), and the article, Hughes et al. (2005).

Definition 3.3.1 (Knot Vectors)**.** A knot vector in one dimension is a non-decreasing set of coordinates in the parameter space, written $\Xi = \{\xi_1, \xi_2, \ldots, \xi_{n+p+1}\}$, where $\xi_i \in \mathbb{R}$ is the ith knot, i is the knot index, $i = 1, 2, \ldots, n + p + 1$. p is the polynomial order, and n is the number of basis functions used to construct the B-spline curve. The knots partition the parameter space into elements.

Knot values may be repeated (referred to as multiplicities), and these multiplicities have important implications for the properties of the basis. If the knots are equally spaced, then the knot vector is said to be uniform, and non-uniform otherwise. And a knot vector is referred to as open, if the first and last knots have a multiplicity of $p + 1$.

Definition 3.3.2 (Univariate B-Spline Basis Functions)**.** With a knot vector in hand, the B-spline basis functions are defined recursively starting with piecewise constants

$(p = 0)$:

$$N_{i,0}(\xi) = \begin{cases} 1 & \text{if } \xi_i \leqslant \xi < \xi_{i+1}, \\ 0 & \text{otherwise.} \end{cases} \tag{3.10}$$

For $p = 1, 2, 3, \ldots$, they are defined by

$$N_{i,p}(\xi) = \frac{\xi - \xi_i}{\xi_{i+p} - \xi_i} N_{i,p-1}(\xi) + \frac{\xi_{i+p+1} - \xi}{\xi_{i+p+1} - \xi_{i+1}} N_{i+1,p-1}(\xi)\,. \tag{3.11}$$

This is referred to as the Cox-de Boor recursion formula.

The results of applying (3.10) and (3.11) to a uniform knot vector are presented in Figure 3.1. Using non-uniform knot vectors makes it possible to obtain much richer behaviour than is possible with simple uniform knot vectors. Figure 3.2, is generated from the quadratic non-uniform knot vector given by $\Xi = \{0, 0, 0, 1, 2, 3, 4, 4, 5, 5, 5\}$. In Figure 3.2, the basis functions are interpolatory at the ends of the interval and at the repeated knot $\xi = 4$, where the functions are C^0-continuous. Everywhere else, the functions are C^1-continuous.

In general, basis functions with order p are C^{p-m_i}-continuous at knots with multiplicity m_i. If m_i happens to be equal to p at say, ξ_i, then the basis function is interpolatory at ξ_i. With a multiplicity of $p + 1$, the basis becomes discontinuous and a patch boundary is formed at that knot.

Definition 3.3.3 (B-spline Curve)**.** Given n basis functions, $N_{i,p}$, $i = 1, 2, \ldots, n$, and corresponding control points $\mathbf{B}_i \in \mathbb{R}^d$, $i = 1, 2, \ldots, n$, a piecewise polynomial B-spline curve is given by

$$\mathbf{C}(\xi) = \sum_{i=1}^{n} N_{i,p}(\xi)\mathbf{B}_i\,. \tag{3.12}$$

Piecewise linear interpolation of the control points gives the control polygon, see Figure 3.3(a). The control points are basically vector valued coefficients of the basis

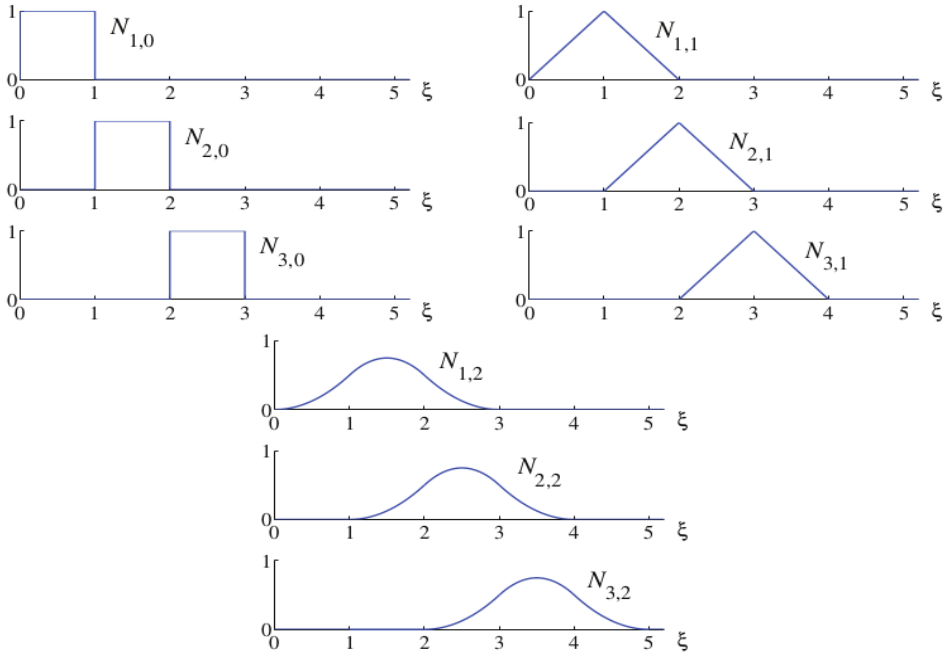

Figure 3.1: Basis functions of order 0, 1, and 2 for uniform knot vector $\Xi = \{0, 1, 2, 3, 4, \ldots\}$ (Cottrell et al. (2009)).

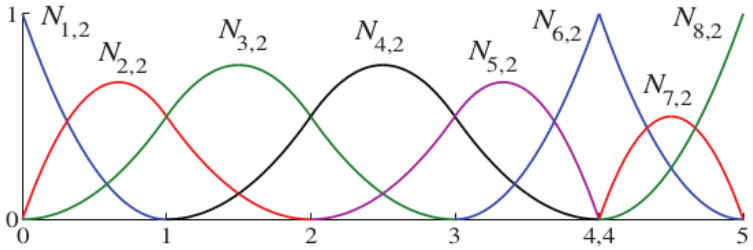

Figure 3.2: Quadratic basis functions for open, non-uniform knot vector $\Xi = \{0, 0, 0, 1, 2, 3, 4, 4, 5, 5, 5\}$ (Cottrell et al. (2009)).

functions and in this sense, they are similar to nodal coordinates in finite element analysis.

The properties of B-spline curves mainly follow from the properties of their basis functions. Piegl and Tiller (1997), discusses many such properties in detail.

Definition 3.3.4 (B-spline Surface)**.** Given a control net $\{\mathbf{B}_{i,j}\}$, $i = 1, 2, \ldots, n$, $j = 1, 2, \ldots, m$, polynomial orders p and q, and knot vectors $\Xi = \{\xi_1, \xi_2, \ldots, \xi_{n+p+1}\}$, and

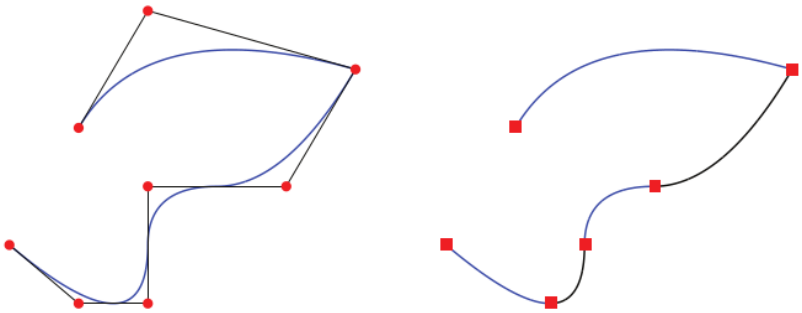

(a) Curve and control points (b) Curve and mesh denoted by knot locations

Figure 3.3: Example of a B-spline, piecewise quadratic curve in $\mathbb{R}^2$. Basis functions and knot vectors as in Figure (3.2) (Cottrell et al. (2009)).

$\mathcal{H} = \{\eta_1, \eta_2, \ldots, \eta_{m+q+1}\}$, a tensor product B-spline surface is defined by

$$\mathbf{S}(\xi, \eta) = \sum_{i=1}^{n} \sum_{j=1}^{m} N_{i,p}(\xi) M_{j,q}(\eta) \mathbf{B}_{i,j}, \tag{3.13}$$

where $N_{i,p}$ and $M_{j,q}$ are univariate B-spline basis functions of order p and q, corresponding to knot vectors Ξ and $\mathcal{H}$, respectively.

In Figure 3.4, an example of B-spline surface and the corresponding control net is shown.

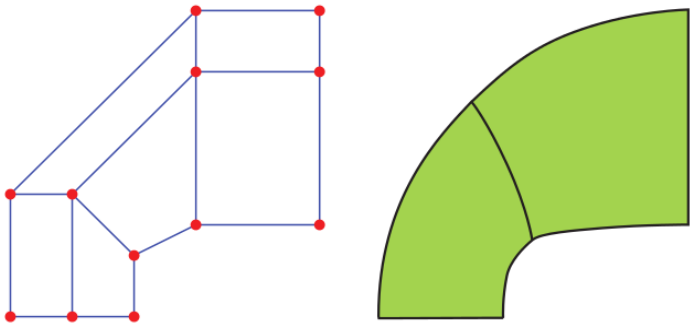

Control net Mesh

Figure 3.4: The control net and mesh for the bi-quadratic B-spline surface with $\Xi = \{0, 0, 0, 0.5, 1, 1, 1\}$ and $\mathcal{H} = \{0, 0, 0, 1, 1, 1\}$ (Cottrell et al., 2009).

Tensor product B-spline solids are defined in an analogous fashion to B-spline surfaces.

Definition 3.3.5 (B-spline Solid)**.** Given a control lattice $\{\mathbf{B}_{i,j,k}\}$, $i = 1, 2, \ldots, n$, $j = 1, 2, \ldots, m$, $k = 1, 2, \ldots, l$, polynomial orders p, q and r, and knot vectors $\Xi = \{\xi_1, \xi_2, \ldots, \xi_{n+p+1}\}$, $\mathcal{H} = \{\eta_1, \eta_2, \ldots, \eta_{m+q+1}\}$, and $\mathcal{Z} = \{\zeta_1, \zeta_2, \ldots, \zeta_{l+r+1}\}$, a B-spline solid is defined by

$$\mathbf{S}(\xi, \eta, \zeta) := \sum_{i=1}^{n} \sum_{j=1}^{m} \sum_{k=1}^{l} N_{i,p}(\xi) M_{j,q}(\eta) L_{k,r}(\zeta) \mathbf{B}_{i,j,k} \,. \tag{3.14}$$

3.3.1 Refinement Strategies

There are a number of ways to enrich B-spline basis while leaving the underlying geometry and its parameterization unchanged. The basic mechanisms of B-spline refinement have subtle differences with their finite element counterparts and these lead to a richer overall refinement space Cottrell et al. (2009).

Knot Insertion

Let $\Xi = \{\xi_1, \xi_2, \ldots, \xi_{n+p+1}\}$, be a knot vector and let $\overline{\xi} \in [\xi_k, \xi_{k+1}[$ be a desired knot. Then, a new $(n+1)$ basis can be formed using the recursion formulas (3.10) and (3.11), with the new knot vector $\Xi = \{\xi_1, \xi_2, \ldots, \xi_k, \overline{\xi}, \xi_{k+1}, \ldots, \xi_{n+p+1}\}$. The new $(n+1)$ control points, $\{\overline{B}_1, \overline{B}_2, \ldots, \overline{B}_{n+1}\}$, can be obtained from the original control points, $\{B_1, B_2, \ldots, B_n\}$ by

$$\overline{B}_i = \alpha_i B_i + (1 - \alpha_i) B_{i-1} \,, \tag{3.15}$$

where

$$\alpha_i = \begin{cases} 1, & 1 \leqslant i \leqslant k - p, \\ \frac{\overline{\xi} - \xi_i}{\xi_{i+p} - \xi_i}, & k - p + 1 \leqslant i \leqslant k, \\ 0, & k + 1 \leqslant i \leqslant n + p + 2. \end{cases} \tag{3.16}$$

Knot insertion is analogous to h-refinement, and can be carried out such that the curve is unchanged, geometrically or parametrically. Existing knot values can be repeated, but in doing so, the continuity of the basis may be reduced.

Order Elevation

Order elevation is the equivalent of p-refinement in finite element analysis, and can be carried out without changing the geometry or its parameterization. Each unique knot value in the knot vector Ξ must be repeated to preserve the discontinuities in the pth derivative of the curve being elevated. The number of new control points introduced due to order elevation, depend on the multiplicities of the existing knots.

k-refinement

k-refinement is a consequence of the non-commutative nature of the order in which order elevation and knot insertions are carried out. That is, if knot insertion is carried out on a given knot vector followed by order elevation, the resulting knot vector will not be the same, in terms of the continuity at the knots, as the knot vector produced when order elevation is first carried out before knot insertion. The latter procedure is what is referred to as k-refinement and has no analogue in standard finite element analysis. In Hughes et al. (2005), the advantages of k-refinement are outlined with an example for the 1-dimensional case.

3.3.2 Non-Uniform Rational B-Splines (NURBS)

There are some desired geometric objects in $\mathbb{R}^d$ that can not be constructed directly using B-splines. These can however, be obtained by projective transformations of B-spline entities in $\mathbb{R}^{d+1}$, $d = 1, 2, 3$. In particular, circles and ellipses, and conic sections in general, can be exactly constructed by projective transformations of piecewise quadratic curves, see Figure 3.5.

The projective transformation of a B-spline curve yields a rational polynomial of the form $C_R(\xi) = f(\xi)/g(\xi)$, where f and g are piecewise polynomials. The construction

of a rational B-spline curve in $\mathbb{R}^d$ proceeds as follows.

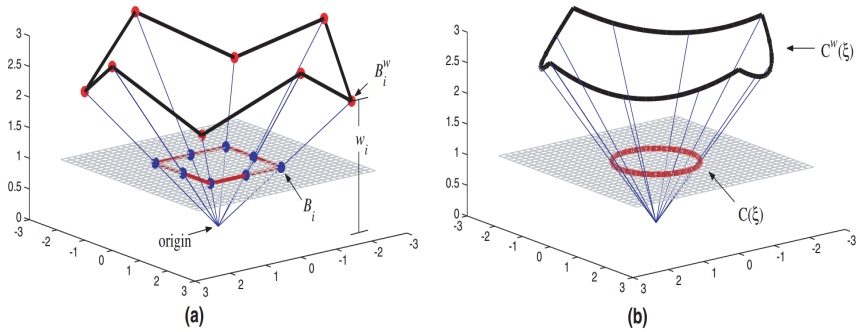

Figure 3.5: Circle in R^2 constructed by projective transformation of piecewise quadratic B-spline in R^3. (a) Projective transformation of "projective control points" yields control points. Weight w_i is the z-component of $\{\mathbf{B}_i^w\}$. (b) Projective transformation of B-spline curve $C^w(\xi)$ yields curve $C(\xi)$. (Hughes et al. (2005)).

Let $\{\mathbf{B}_i^w\}$ be a set of control points for a B-spline curve in R^{d+1} with knot vector Ξ, also referred to as the "projective" control points for the NURBS curve in R^d. The following relations are used to obtain the control points in R^d from the projective control points:

$$(\mathbf{B}_i)_j = (\mathbf{B}_i^w)_j / w_i, \quad j = 1, 2, \ldots, d, \tag{3.17}$$

$$w_i = (\mathbf{B}_i^w)_{d+1}. \tag{3.18}$$

Where $(\mathbf{B}_i)_j$ is the jth component of the vector $\mathbf{B}_i$, etc. and w_i is the ith weight. The weighting function W is defined as

$$W(\xi) = \sum_{i=1}^{n} N_{i,p}(\xi) w_i \,, \tag{3.19}$$

where $N_{i,p}(\xi)$ is the standard B-spline basis function.

In Figure 3.5(a), the weights are the vertical coordinates of the control points defining the piecewise quadratic B-spline curve in R^3. Then, the rational basis functions and NURBS curve are defined as

$$R_i^p(\xi) = \frac{N_{i,p}(\xi) w_i}{\sum_{i=1}^{n} N_{i,p}(\xi) w_i} = \frac{N_{i,p}(\xi) w_i}{W(\xi)}, \quad \text{and,} \tag{3.20}$$

$$\mathbf{C}(\xi) = \sum_{i=1}^{n} R_i^p(\xi)\mathbf{B}_i \,. \tag{3.21}$$

Analogously, rational surfaces and solids are given, respectively, in terms of the rational basis functions as

$$R_{i,j}^{p,q}(\xi,\eta) = \frac{N_{i,p}(\xi)M_{j,q}(\eta)w_{i,j}}{\sum_{\hat{i}=1}^{n}\sum_{\hat{j}=1}^{m} N_{\hat{i},p}(\xi)M_{\hat{j},q}(\eta)w_{\hat{i},\hat{j}}} \,, \tag{3.22}$$

$$R_{i,j,k}^{p,q,r}(\xi,\eta,\zeta) = \frac{N_{i,p}(\xi)M_{j,q}(\eta)L_{k,r}(\zeta)w_{i,j,k}}{\sum_{\hat{i}=1}^{n}\sum_{\hat{j}=1}^{m}\sum_{\hat{k}=1}^{l} N_{\hat{i},p}(\xi)M_{\hat{j},q}(\eta)L_{\hat{k},r}(\zeta)w_{\hat{i},\hat{j},\hat{k}}} \,. \tag{3.23}$$

3.3.3 NURBS as a Basis for Analysis

Over the years, NURBS have remained the mainstay of geometric design due to their flexibility and precision. In this section they are discussed in the setting of analysis where their unique properties have been shown to be ideally suited. NURBS have generalized and provided an improvement to the traditional piecewise polynomial basis functions, yielding more accuracy and robustness across a wide array of applications (Cottrell et al., 2009).

The Isoparametric Concept

The use of the same basis for both geometry and analysis is referred to as the isoparametric concept. In classical finite element analysis, the isoparametric concept is characterized by the use of the basis chosen to approximate the unknown solution fields, to also approximate the known geometry. Isogeometric analysis on the other hand, involves the use of a basis capable of exactly representing the known geometry, which is then used as a basis for the fields to be approximated. This logical shift makes it possible to utilize all of the information that are present in a problem.

Several theorems regarding convergence for NURBS based isogeometric analysis have been shown in Bazilevs et al. (2006). The most basic convergence requirements in

many numerical methods can be achieved by a reasonably smooth isoparametric basis that is also a partition of unity. Conditions which NURBS have been shown to satisfy. According to Hughes (2000), basis that satisfy the following,

1. C^1 on the element interiors,

2. C^0 on the element boundaries,

3. complete,

are sufficiently equipped to obtain basic convergence proofs for a wide class of problems.

The first two requirement are satisfied by most basis one might consider in numerical methods. The third condition, requires that, on any given element K, the basis be capable of representing all linear functions. That is, given a basis $\{N_a\}_{a=1}^{n_{en}}$ (n_{en}, being the number of "element nodes" in K) for the solution space, completeness demands that there exist coefficients d_a such that, for arbitrary constants C_0, C_1, C_2, and C_3,

$$u_h|_K \equiv \sum_{a=1}^{n_{en}} N_a d_a = C_0 + C_1 x + C_2 y + C_3 z. \tag{3.24}$$

The last property has been found to be satisfied by any isoparametric basis that is also a partition of unity. This can be seen by noting that, for each point $\mathbf{x} \in K$ there exists a parameter ξ such that

$$\mathbf{x}(\xi) \equiv \left\{ \begin{array}{c} x(\xi) \\ y(\xi) \\ z(\xi) \end{array} \right\} = \sum_{a=1}^{n_{en}} N_a(\xi) \left\{ \begin{array}{c} x_a \\ y_a \\ z_a \end{array} \right\}, \tag{3.25}$$

where x_a, y_a and z_a are the components of the ath vector-valued coefficient defining the geometry in element K. Now, as the basis is a partition of unity, at that same

point ξ we have

$$\sum_{a=1}^{n_{en}} N_a(\xi) \equiv 1 \,. \tag{3.26}$$

Inserting (3.25) and (3.26) into (3.24) and solving for d_a gives

$$d_a = C_0 + C_1 x_a + C_2 y_a + C_3 z_a \,. \tag{3.27}$$

Thus, the isoparametric concept and the partition of unity sufficiently ensure completeness. In addition, they are essential to ensuring that isogeometric analysis will result in convergent methods for varying choices of element technology, NURBS included.

Taking the $N_a(\xi)$'s as NURBS functions, and $\{x_a, y_a, z_a\}^T$ as the components of a control point $\mathbf{B}_a$, $\Phi : \widehat{\Omega} \to \Omega$ defines a geometrical mapping, and other functions can be built over the entire parametric domain in a similar way. For instance, let $\widehat{u}_h : \widehat{\Omega} \to \mathbb{R}$ be defined by

$$\widehat{u}_h(\xi) \equiv \sum_{A=1}^{n_{np}} N_A(\xi) d_A \,. \tag{3.28}$$

n_{np} is the total number of control variables (nodes or knots) in the domain. The d_A are the control variables and as with control points, the non-interpolatory nature of the basis prevents strictly interpreting the control variables as can be done for nodal values in FEA. The function then can be defined over the physical domain by considering a composition with the inverse of the geometrical mapping, such that, $u_h : \Omega \to \mathbb{R}$ is given by;

$$u_h = \widehat{u}_h(\xi) \circ \Phi^{-1} \,. \tag{3.29}$$

Due to the fact that the geometrical mapping is invertible, u_h is usually used to refer to the function irrespective of the coordinates being used (that is, physical or

parametric domain). The properties of u_h, such defined, follow from those of the basis. Refinement of the basis can also be carried out without affecting the geometry or its parameterization.

3.4 The Model Biharmonic Problem

Let us consider as a model problem the biharmonic equation.

Find $u : \overline{\Omega} \subset \mathbb{R}^d \to \mathbb{R}$, $d = 1, 2, 3$, such that

$$\left.\begin{array}{rll} \Delta^2 u = f & \text{in } \Omega, & \\ \left.\begin{array}{rl} u = g_0 & \text{on } \Gamma_D, \\ \mathbf{n}\cdot\nabla u = g_1 & \text{on } \Gamma_D, \end{array}\right\} & \text{Dirichlet boundary conditions,} & \\ \left.\begin{array}{rl} \Delta u = g_2 & \text{on } \Gamma_N, \\ \mathbf{n}\cdot\nabla\Delta u = g_3 & \text{on } \Gamma_N, \end{array}\right\} & \text{Neumann boundary conditions,} & \end{array}\right\} \tag{3.30}$$

where $\overline{\Gamma_D \bigcup \Gamma_N} = \Gamma = \partial\Omega$, $\Gamma_D \bigcap \Gamma_N = \varnothing$, and $\mathbf{n}$ is the unit outward normal vector on $\partial\Omega$. The functions f, g_0, g_1, g_2, g_3, are all given.

For sufficiently smooth domain, and under certain restrictions on $g_0, \ldots, g_3$, a unique solution is known to exist.

3.4.1 The Variational Formulation

The technique begins by defining a weak (variational) counterpart of (3.30).

To obtain the weak formulation, multiply through (3.30)(a) by a test function v, integrate by parts and incorporate the pertinent boundary conditions.

$$\int_\Omega f v \,\mathrm{d}\Omega = \int_\Omega (\Delta^2 u) v \,\mathrm{d}\Omega\,. \tag{3.31}$$

In (3.31), since $\Delta^2 u = \Delta\Delta u$, let $\Delta u = w$.

Replacing ω in (3.9) by w and φ by v and integrating, and using (3.7) gives

$$\int_\Omega (\Delta w) v \,\mathrm{d}\Omega + \int_\Omega \nabla v \cdot \nabla w \,\mathrm{d}\Omega = \int_\Omega \nabla \cdot (v \nabla w) \,\mathrm{d}\Omega,$$

$$= \int_{\partial\Omega} v(\mathbf{n} \cdot \nabla w)\, \mathrm{d}\Gamma\,.$$

Using the substitution $\Delta u = w$ gives

$$\int_\Omega (\Delta^2 u) v \, \mathrm{d}\Omega + \int_\Omega \nabla v \cdot \nabla \Delta u \, \mathrm{d}\Omega = \int_{\partial\Omega} v(\mathbf{n} \cdot \nabla \Delta u)\, \mathrm{d}\Gamma\,. \tag{3.32}$$

Next, let $\varphi = \Delta u$ and $\omega = v$. By using (3.9),

$$\nabla \cdot (\Delta u \nabla v) = \nabla \Delta u \cdot \nabla v + \Delta u \Delta v.$$

Taking integrals, and applying (3.7) again gives

$$\begin{aligned}\int_\Omega \Delta u \Delta v \, \mathrm{d}\Omega + \int_\Omega \nabla \Delta u \cdot \nabla v \, \mathrm{d}\Omega &= \int_{\partial\Omega} \nabla \cdot (\Delta u \nabla v)\, \mathrm{d}\Omega, \\ &= \int_{\partial\Omega} \Delta u (\mathbf{n} \cdot \nabla v)\, \mathrm{d}\Gamma\,. \end{aligned} \tag{3.33}$$

Substituting (3.33) into (3.32) gives

$$\int_\Omega (\Delta^2 u) v \, \mathrm{d}\Omega - \int_\Omega \Delta u \Delta v \, \mathrm{d}\Omega + \int_{\partial\Omega} \Delta u (\mathbf{n} \cdot \nabla v)\, \mathrm{d}\Gamma = \int_{\partial\Omega} v(\mathbf{n} \cdot \nabla \Delta u)\, \mathrm{d}\Gamma\,.$$

Which can be rewritten as

$$\int_\Omega (\Delta^2 u) v \, \mathrm{d}\Omega = \int_\Omega \Delta u \Delta v \, \mathrm{d}\Omega + \int_{\partial\Omega} v(\mathbf{n} \cdot \nabla \Delta u)\, \mathrm{d}\Gamma - \int_{\partial\Omega} \Delta u (\mathbf{n} \cdot \nabla v)\, \mathrm{d}\Gamma\,.$$

Thus, from (3.31), we now have

$$\int_\Omega f v \, \mathrm{d}\Omega = \int_\Omega \Delta u \Delta v \, \mathrm{d}\Omega + \int_{\partial\Omega} v(\mathbf{n} \cdot \nabla \Delta u)\, \mathrm{d}\Gamma - \int_{\partial\Omega} \Delta u (\mathbf{n} \cdot \nabla v)\, \mathrm{d}\Gamma\,.$$

Substituting for the appropriate boundary conditions, $\forall v \in V_0$,

$$\int_\Omega f v \, \mathrm{d}\Omega = \int_\Omega \Delta u \Delta v \, \mathrm{d}\Omega + \int_{\Gamma_N} v g_3 \, \mathrm{d}\Gamma - \int_{\Gamma_N} g_2 (\mathbf{n} \cdot \nabla v)\, \mathrm{d}\Gamma\,.$$

The variational or weak formulation of (3.30) reads as follows:

Find $u \in V_g$, such that

$$a(u, v) = l(v), \quad \forall v \in V_0, \tag{3.34}$$

where, the bilinear form and linear form are given by

$$a(u,v) = \int_\Omega \Delta u \Delta v \, \mathrm{d}\Omega \quad \text{and} \quad l(v) = \int_\Omega f v \, \mathrm{d}\Omega - \int_{\Gamma_N} v g_3 \, \mathrm{d}\Gamma + \int_{\Gamma_N} g_2 (\mathbf{n} \cdot \nabla v) \, \mathrm{d}\Gamma,$$

respectively.

The hyperplane V_g and test space V_0 are given by

$$V_g := \{u : u \in H^2(\Omega), u|_{\Gamma_D} = g_0, \, \mathbf{n} \cdot \nabla u|_{\Gamma_D} = g_1\},$$

$$V_0 := \{v : v \in H^2(\Omega), v|_{\Gamma_D} = 0, \, \mathbf{n} \cdot \nabla v|_{\Gamma_D} = 0\}.$$

It is clear that $a(\cdot, \cdot)$ is symmetric. The solution to (3.34) is called a weak solution.

Existence, Uniqueness and Stability

Next, it is shown that the weak solution exists and is unique. The following theorem provides the conditions necessary for the existence and uniqueness of the weak solution to the model problem.

Theorem 3.4.1 (Lax-Milgram Lemma)**.** *Let V be a Hilbert space, let $a(\cdot, \cdot) : V \times V \longrightarrow \mathbb{R}$ be a continuous V-elliptic bilinear form, and let $f : V \longrightarrow \mathbb{R}$ be a continuous linear form.*

Then the abstract variational problem: Find an element u such that

$$u \in V \quad \textit{and} \quad \forall v \in V, \quad a(u,v) = f(v),$$

has one and only one solution.

Proof. See (Ciarlet, 2002, Theorem 1.1.3). □

In the following theorem, using Theorem 3.4.1, it is shown that the variational form (3.34), obtained for problem (3.30), has a unique solution.

Theorem 3.4.2 (Lax-Milgram)**.** *Let V be a Hilbert space with inner product $(\cdot, \cdot)$ and $V_0 \subset V$. Let $a(\cdot, \cdot) : V \times V \longrightarrow \mathbb{R}$ be a bilinear form satisfying*

1. *bounded/continuous :* $|a(u,v)| \leqslant \mu_b \|u\|_V \|v\|_V$ *with* $\mu_b > 0$, $\forall u, v \in V$,

2. *coercive/V-elliptic :* $a(v,v) \geqslant \mu_c \|v\|_V, \quad \mu_c > 0$, $\forall v \in V$.

Then, for any given $g_0, g_1, g_2, g_3 \in V$ *and* $l(\cdot) \in V_0^*$, *the variational problem: find* $u \in g_i + V_0$, $i = 0, \ldots, 3$, *such that*

$$a(u,v) = l(v),\ \forall v \in V_0,$$

has a unique solution $u \in g_i + V_0$ *which fulfills the a-priori estimate*

$$\|u\|_V \leqslant \frac{1}{\mu_b} \|l\|_{V_0^*} + \left(1 + \frac{\mu_b}{\mu_c}\right) \| \sum_{i=0}^{3} g_i \|_V \,. \tag{3.35}$$

Proof. 1. First, the boundedness of the bilinear form is shown by using Cauchy-Schwarz's inequality as follows.

$$\begin{aligned} |a(u,v)| &= \left| \int_\Omega \Delta u \Delta v \, \mathrm{d}\Omega \right| \\ &\leqslant \left(\int_\Omega |\Delta u|^2 \, \mathrm{d}\Omega \right)^{\frac{1}{2}} \left(\int_\Omega |\Delta v|^2 \, \mathrm{d}\Omega \right)^{\frac{1}{2}} \\ &= \|\Delta u\|_{L^2(\Omega)} \|\Delta v\|_{L^2(\Omega)} \\ &\leqslant \|\Delta u\|_V \|\Delta v\|_V \,. \end{aligned}$$

2. Next, it is shown that the bilinear form $a(\cdot,\cdot)$ is coercive.

$$a(v,v) = \int_\Omega \Delta v \Delta v \, \mathrm{d}\Omega = \|\Delta v\|^2_{L^2(\Omega)}. \tag{3.36}$$

Then, by the definition of the norm on V and the Poincaré-Friedrichs' inequality (3.6),

$$\begin{aligned} \|v\|_V^2 &= \|v\|^2_{L^2(\Omega)} + \|\nabla v\|^2_{L^2(\Omega)} + \|\Delta v\|^2_{L^2(\Omega)} \\ &\leqslant C_1^2 \|\Delta v\|^2_{L^2(\Omega)} + \|\Delta v\|^2_{L^2(\Omega)} = (1 + C_1^2) \|\Delta v\|^2_{L^2(\Omega)} \,. \end{aligned}$$

Thus

$$\|\Delta v\|^2_{L^2(\Omega)} \geqslant \frac{1}{1+C_1^2}\|v\|^2_V \,. \tag{3.37}$$

Therefore

$$a(v,v) \geqslant \mu_c \|v\|^2_V \,, \text{ with } \mu_c = \frac{1}{(1+C_1^2)} \,. \tag{3.38}$$

□

3.4.2 Galerkin's Method

Galerkin's method involves constructing finite-dimensional approximations of V_g and V_0, which will be denoted by $V_{g,h}$ and $V_{0,h}$, respectively, such that $V_{g,h} \subset V_g$ and $V_{0,h} \subset V_0$.

Using the Bubnov-Galerkin approach, it is only necessary to obtain a finite dimensional approximation to V_0, since it is assumed that there is a given function $g_h \in V_{g,h}$ such that $g_h|_{\Gamma_D} = g_0$ and $\mathbf{n} \cdot \nabla g_h|_{\Gamma_D} = g_1$, thus, for every $u_h \in V_{g,h}$ there exists a unique $w_h \in V_{0,h}$ such that

$$u_h = w_h + g_h. \tag{3.39}$$

With this, the Galerkin form of (3.34) can be written as:

Given g_h, g_2, g_3, find $u_h = w_h + g_h$, where $w_h \in V_{0,h}$, such that for all $v_h \in V_{0,h}$,

$$a(u_h, v_h) = l(v_h). \tag{3.40}$$

Making the substitution for u_h, and rearranging gives

$$\int_\Omega \Delta(w_h + g_h)\Delta v_h \,\mathrm{d}\Omega = \int_\Omega f v_h \,\mathrm{d}\Omega - \int_{\Gamma_N} g_3 v_h \,\mathrm{d}\Gamma + \int_{\Gamma_N} g_2(\mathbf{n}\cdot\nabla v_h)\,\mathrm{d}\Gamma,$$

$$\int_\Omega \Delta w_h \Delta v_h \,\mathrm{d}\Omega + \int_\Omega \Delta g_h \Delta v_h \,\mathrm{d}\Omega = \int_\Omega f v_h \,\mathrm{d}\Omega - \int_{\Gamma_N} g_3 v_h \,\mathrm{d}\Gamma + \int_{\Gamma_N} g_2(\mathbf{n}\cdot\nabla v_h)\,\mathrm{d}\Gamma,$$

$$\int_{\Omega} \Delta w_h \Delta v_h \, \mathrm{d}\Omega = \int_{\Omega} f v_h \, \mathrm{d}\Omega - \int_{\Gamma_N} g_3 v_h \, \mathrm{d}\Gamma + \int_{\Gamma_N} g_2 (\mathbf{n} \cdot \nabla v_h) \, \mathrm{d}\Gamma - \int_{\Omega} \Delta g_h \Delta v_h \, \mathrm{d}\Omega. \tag{3.41}$$

Thus, from (3.41),

$$a(w_h, v_h) = l(v_h) - a(g_h, v_h). \tag{3.42}$$

Which, since $a(\cdot, \cdot)$ is symmetric, can be rewritten as

$$a(v_h, w_h) = l(v_h) - a(v_h, g_h). \tag{3.43}$$

3.4.3 Convergence and Error Estimates

In Tagliabue et al. (2014), the authors extended the results in Bazilevs et al. (2006), which provided the intermediate results and the error estimates for the solution of second order elliptic problems using the Galerkin method, to the solution of elliptic problems of order $2m$, with $m > 1$. This necessitates introducing some new notation.

Let $\Xi = \{\xi_1, \xi_2, \ldots, \xi_{n+p+1}\}$ be a knot vector, where ξ_i is the i-th knot, with the knot index $i \in \{1, \ldots, n+p+1\}$ characterized by the polynomial degree p and the number of basis functions n defining the B-spline basis, respectively. By convention, it is assumed that $\xi_1 = 0$ and $\xi_{n+p+1} = 1$, such that the parametric domain is defined as $\widehat{\Omega} := (\xi_1, \xi_{n+p+1}) = (0, 1) \subset \mathbb{R}$.

Let r be the number of distinct knots in Ξ and $\mathcal{Z}$ be the collection of the ordered distinct knots of Ξ. That is, $\mathcal{Z} = \{\zeta_1, \ldots, \zeta_r\}$, with $\zeta_1 = \xi_1 = 0$ and $\zeta_r = \xi_{n+p+1} = 1$.

Now, it is possible to define the concept of mesh elements in $\widehat{\Omega}$. Let $\widehat{\mathcal{K}}_h$ be a one-dimensional mesh over $\widehat{\Omega}$, that is, the collection of sub-domains bounded by two

distinct knots, that is

$$\widehat{\mathcal{K}}_{\widehat{h}} := \{\widehat{K} = (\zeta_j, \zeta_{j+1}) : j = 1, \ldots, r-1\}. \tag{3.44}$$

Let $\widehat{h} := \max\{\widehat{h}_{\widehat{K}} : \widehat{K} \in \widehat{\mathcal{K}}_h\}$ be the global mesh size in $\widehat{\Omega}$, where $\widehat{h}_{\widehat{K}} := diam(\widehat{K})$, $\widehat{K} \in \widehat{\mathcal{K}}_h$. Let $\mathcal{M} := \{m_1, \ldots, m_r\}$, be a vector storing the multiplicities of the knots in $\mathcal{Z}$, where $m_j \geqslant 1$, represents the multiplicity of the knot value ζ_j, $\; j = 1, \ldots, r$.

Since the basis functions are point-wise non-negative and C^∞-continuous everywhere except in the knot values ζ_j, where they are C^{p-m_j}-continuous, it is convenient to define the vector $\mathbb{K} = \{k_1, \ldots, k_r\}$, containing the smoothness integer parameters $k_j = p - m_j + 1$, $\; j = 1, \ldots, r$, such that $0 \leqslant k_j \leqslant p$. Let $k_{min} := \min_{j=2,\ldots,r-1}\{k_j\}$ be the minimum smoothness parameter. With this, in the knot ζ_j, the basis functions are C^{k_j-1}-continuous.

Let $\widehat{\mathcal{S}}_h := span\{\widehat{N}_i\}_{i=1}^n$, be the B-spline space built from the basis functions in $\widehat{\Omega}$. $\widehat{N}_i : \widehat{\Omega} \longrightarrow \mathbb{R}$, for $i = 1, \ldots, n$, are built as described in section 3.3, and the B-splines in $\widehat{\mathcal{S}}_h$ are globally $C^{k_{min}-1}$-continuous.

Extending these to the d-dimensional case gives; $\Xi_\alpha = \{\xi_1^\alpha, \xi_2^\alpha, \ldots, \xi_{n_\alpha+p_\alpha+1}^\alpha\}$ for $\alpha = 1, \ldots, d$. $\mathcal{Z}_\alpha = \{\zeta_1^\alpha, \ldots, \zeta_{r_\alpha}^\alpha\}$, $\; \mathcal{M}_\alpha := \{m_1^\alpha, \ldots, m_{r_\alpha}^\alpha\}$, $\quad \mathbb{K}_\alpha = \{k_1^\alpha, \ldots, k_{r_\alpha}^\alpha\}$, and the minimum integer parameter $k_{min}^\alpha := \min_{j_\alpha=2,\ldots,r_\alpha-1}\{k_{j_\alpha}^\alpha\}$.

Then a mesh $\widehat{\mathcal{K}}_h$ in $\widehat{\Omega} = (0,1)^d$ is defined by its partition into d-dimensional elements: $\widehat{\mathcal{K}}_h = \{\widehat{K} := \otimes_{\alpha=1}^d(\zeta_{j_\alpha}^\alpha, \zeta_{j_\alpha+1}^\alpha), 1 \leqslant j_\alpha \leqslant r_\alpha - 1\}$, with element size $\widehat{h}_{\widehat{K}} = diam(\widehat{K})$, $\quad \forall \widehat{K} \in \widehat{\mathcal{K}}_h$, and global mesh size $\widehat{h} := \max_{\widehat{K}\in\widehat{\mathcal{K}}_h}\{\widehat{h}_{\widehat{K}}\}$.

For each multi-index $\mathbf{i} := (i_1, \ldots, i_d)$ in the set $I = \{\mathbf{i} = (i_1, \ldots, i_d) : 0 \leqslant i_\alpha \leqslant$

n_α for $1 \leqslant \alpha \leqslant d\}$, the multivariate B-spline basis functions are given by

$$\widehat{N}_{\mathbf{i}} : \widehat{\Omega} \longrightarrow \mathbb{R}, \quad \widehat{N}_{\mathbf{i}}(\boldsymbol{\eta}) := \prod_{\alpha=1}^{d} \widehat{N}_{i_\alpha}^{\alpha}(\eta_\alpha), \tag{3.45}$$

with the corresponding B-spline basis function space being; $\widehat{\mathcal{S}}_h := span\{\widehat{N}_{\mathbf{i}}\}_{\mathbf{i}\in I}$.

To obtain the NURBS basis functions on $\widehat{\Omega} = (0,1)^d$, define the weighting functions as

$$W : \widehat{\Omega} \longrightarrow \mathbb{R}, \quad W(\boldsymbol{\eta}) := \sum_{\mathbf{i}\in I} \omega_{\mathbf{i}} \widehat{N}_{\mathbf{i}}(\boldsymbol{\eta}), \tag{3.46}$$

with the $\mathbf{i}$th multivariate NURBS basis given as

$$\widehat{R}_{\mathbf{i}} : \widehat{\Omega} \longrightarrow \mathbb{R}, \quad \widehat{R}_{\mathbf{i}}(\boldsymbol{\eta}) = \frac{\widehat{N}_{\mathbf{i}}(\boldsymbol{\eta})\omega_{\mathbf{i}}}{W(\boldsymbol{\eta})}, \quad \forall \mathbf{i} \in I, \tag{3.47}$$

and the corresponding NURBS space is $\widehat{V}_h := span\{\widehat{R}_{\mathbf{i}}\}_{\mathbf{i}\in I}$.

For the set of control points $\{\mathbf{B}_{\mathbf{i}}\}_{\mathbf{i}\in I} \subseteq \mathbb{R}^d$, the following geometrical mapping from $\widehat{\Omega}$ (parametric space) to Ω (physical space) is given.

$$\Phi : \widehat{\Omega} \longrightarrow \Omega \subseteq \mathbb{R}^d, \quad \text{such that} \quad \Phi(\boldsymbol{\eta}) = \sum_{\mathbf{i}\in I} R_{\mathbf{i}}(\boldsymbol{\eta})\mathbf{B}_{\mathbf{i}}. \tag{3.48}$$

Using this mapping, the physical mesh $\mathcal{K}_h := \{K = \Phi(\widehat{K}) : \widehat{K} \in \widehat{\mathcal{K}}_h\}$ can be defined, with global mesh size $h := \max\{\|\nabla\Phi\|_{L^\infty(\widehat{K})}\widehat{h}_{\widehat{K}} : \widehat{K} \in \widehat{\mathcal{K}}_h\}$.

The NURBS space in Ω is the "push-forward" of $\widehat{V}_h$ in $\widehat{\Omega}$, that is,

$$V_h := span\{\widehat{R}_{\mathbf{i}} \circ \Phi^{-1}\}_{\mathbf{i}\in I} = span\{R_{\mathbf{i}}\}_{\mathbf{i}\in I},$$

where $R_{\mathbf{i}}$ is the NURBS basis in the physical domain.

Remark 3.4.1. *V_h as defined above is equivalent to $V_{0,h}$ defined in section 3.4.2.*

In Bazilevs et al. (2006), the interpolation error estimate was based on the introduction of the *support extension* $\overline{\widehat{K}}$ of an element $\widehat{K}$ of the mesh $\widehat{\mathcal{K}}_h$ in $\widehat{\Omega}$, defined as the union of the supports of basis functions whose support intersect the element $\widehat{K}$. The physical support extension of an element $K = \Phi(\widehat{K})$ of the physical mesh $\mathcal{K}_h$ is then taken as the image of $\overline{\widehat{K}}$ under the geometrical mapping Φ and is denoted by $\overline{K}$, that is, $\overline{K} := \Phi(\overline{\widehat{K}})$.

Given a function $\widehat{v} \in L^2(\widehat{\Omega})$ defined in the parametric domain, the projective operator over $\widehat{\mathcal{S}}_h$, $\Pi_{\widehat{\mathcal{S}}_h}$, is defined as

$$\Pi_{\widehat{\mathcal{S}}_h} : L^2(\widehat{\Omega}) \longrightarrow \widehat{\mathcal{S}}_h, \quad \Pi_{\widehat{\mathcal{S}}_h}\widehat{v} := \sum_{\mathbf{i}\in I} \lambda_{\mathbf{i}}(\widehat{v})\widehat{N}_{\mathbf{i}}, \tag{3.49}$$

where the linear functionals $\lambda_{\mathbf{i}} \in L^{2,*}(\widehat{\Omega})$, determine the dual basis for the set of B-splines ($\lambda_{\mathbf{j}}(\widehat{N}_{\mathbf{i}}) := \delta_{\mathbf{i},\mathbf{j}}$ for $\mathbf{i},\ \mathbf{j}\ \in I$).

The corresponding projective operator over the NURBS space $\widehat{V}_h$ in the parameter domain, $\Pi_{\widehat{h}}$, is defined as

$$\Pi_{\widehat{h}} : L^2(\widehat{\Omega}) \longrightarrow \widehat{V}_h, \quad \Pi_{\widehat{h}}\widehat{v} := \frac{\Pi_{\widehat{\mathcal{S}}_h}(W\widehat{v})}{W}, \quad \forall \widehat{v} \in L^2(\widehat{\Omega}). \tag{3.50}$$

Then, the projective operator over V_h can be defined as

$$\Pi_h : L^2(\Omega) \longrightarrow V_h, \quad \Pi_h v := (\Pi_{\widehat{h}}(\widehat{v})) \circ \Phi^{-1}. \tag{3.51}$$

The following theorem provides the interpolation error estimates for an element K, with respect to its support extension.

Theorem 3.4.3 (Local interpolation error estimates)**.** *Given integers l and s such that $0 \leqslant l \leqslant s \leqslant p+1$ and $s \geqslant m$, for a function $u \in L^2(\Omega) \bigcap H^s(\overline{K})$, the estimate for the local interpolation error reads:*

$$|u - \Pi_h u|_{H^l(K)} \leqslant C_{shape} h_K^{s-l} \sum_{i=0}^{s} \|\nabla \Phi\|^{i-s}_{L^\infty(\widehat{\overline{K}})} \|u\|_{H^i(\overline{K})}, \tag{3.52}$$

where h_K is the element size of $K \in \mathcal{K}_h$ and $\nabla\Phi$ denotes the deformation tensor of the geometrical mapping Φ.

Proof. See [Theorem 3.1 in Tagliabue et al. (2014)]. □

The next couple of propositions provide the global interpolation error estimates for NURBS-based IgA for sufficiently smooth basis.

Proposition 3.4.4. *Given integers l and s such that $0 \leqslant l \leqslant s \leqslant p+1$ and $s \geqslant m$, for a function $u \in H^s(\Omega)$, then*

$$\sum_{K \in \mathcal{K}_h} |u - \Pi_h u|^2_{H^l(K)} \leqslant C_{shape} h^{2(s-l)} \|u\|^2_{H^s(\Omega)}. \tag{3.53}$$

Proof. See [Proposition 3.1 in Tagliabue et al. (2014)]. □

Proposition 3.4.5. *(Global interpolation error estimate.) Under the hypothesis of proposition 3.4.4, if in addition $l \leqslant k_{min}$, then*

$$|u - \Pi_h u|_{H^l(\Omega)} \leqslant C_{shape} h^{s-l} \|u\|^2_{H^s(\Omega)}. \tag{3.54}$$

Proof. See [Proposition 3.2 in Tagliabue et al. (2014)]. □

Corollary 3.4.6. *Let $u \in H^r(\Omega)$ be a function defined in the physical domain Ω. Given an integer l such that $0 \leqslant l \leqslant p+1$, $l \leqslant r$, then*

$$|u - \Pi_h u|_{H^l(\Omega)} \leqslant C_{shape} h^{\delta-l} \|u\|^2_{H^r(\Omega)}, \tag{3.55}$$

where $\delta := \min\{p+1, r\}$

Proof. See [Corollary 3.1 in Tagliabue et al. (2014)]. □

Finally, the next theorem provides the *a-priori* error estimates for elliptic PDEs of order $2m$ with $m \geqslant 1$.

Theorem 3.4.7 (A-priori error estimate in norm H^m)**.** *Let $u \in H^r(\Omega)$ be the exact solution of* (3.34) *and $u_h \in V_h$ the approximation solution obtained with the NURBS-based IgA method with the basis functions of global regularity $k_{min} \geqslant m$. Then, the following a-priori error estimate holds:*

$$\|u - u_h\|_{H^m(\Omega)} \leqslant \overline{C} h^{\gamma} \|u\|_{H^r(\Omega)}, \tag{3.56}$$

where $\gamma := \min\{p+1, r\} - m$ and $\overline{C} := \dfrac{\mu_b}{\mu_c} C_{shape}$.

Proof. See [Theorem 3.2 in Tagliabue et al. (2014)]. □

Chapter 4

Results

4.1 Introduction

In this chapter, a dG-IgA scheme is derived for the biharmonic problem. The existence and uniqueness of the solution to the model problem is shown, and *a-priori* error estimates are presented for the scheme.

4.2 Discontinuous Galerkin Isogeometric Analysis

The discontinuous Galerkin methods provide a framework for working with, or in solution spaces whose functions are not necessarily continuous over patch interfaces. The method has been employed together with Isogeometric analysis to handle multi-patch cases, which occur when dealing with complex and, or multiply connected geometries. The other option for handling multiple patches in Isogeometric analysis is by introducing constraint equations which are imposed strongly as described in Cottrell et al. (2009).

Since the dG methodology is employed to enforce continuity weakly across patch

interfaces for problem (3.30), it is necessary to first define the domain Ω as the union of non-overlapping sub-domains (patches).

Let $\mathcal{T}_h := \{\Omega_i\}_{i=1}^N$, where Ω_i are the sub-domains, $i = \{1, \ldots, N\}$, such that

$$\overline{\Omega} = \bigcup_{i=1}^{N} \overline{\Omega}_i, \qquad \text{with } \Omega_i \bigcap \Omega_j = \varnothing, \text{ if } i \neq j.$$

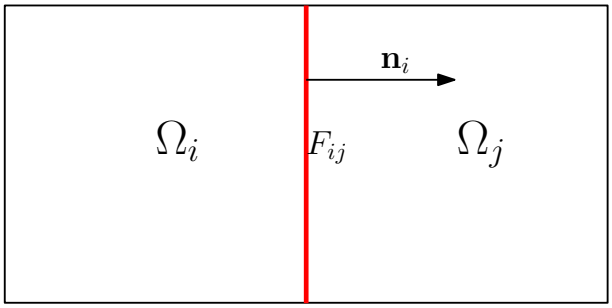

Figure 4.1: An example of a multipatch domain, Ω, with sub-domains or patches, Ω_i, Ω_j, with the corresponding interface and interior unit normal.

Let $F_{ij} = \partial\Omega_i \bigcap \partial\Omega_j$ be the interface between patches Ω_i and Ω_j, and $\mathcal{F}_I$ be the collection of all such interfaces. Let $F_i = \partial\Omega_i \bigcap \partial\Omega$, and $\mathcal{F}_D$ be the collection of all such patch boundaries, and let $\mathcal{F} = \mathcal{F}_I \bigcup \mathcal{F}_D$. It is conventional to assume that the parametric domain, $\widehat{\Omega}$, has unit length, that is, $\widehat{\Omega} = [0,1]^d$, $d = 1, 2, 3$.

Each patch Ω_i is associated with knot vectors, $\Xi_\alpha^{(i)}$, on $\widehat{\Omega}$, $\alpha = 1, \ldots, d$, $i = 1, \ldots, N$, that create a mesh $\widehat{\mathcal{K}}_{h,i} = \{\widehat{K}\}$ (parametric mesh), where $\widehat{K}$ are the elements created by the distinct knot spans in $\Xi_\alpha^{(i)}$, as described in section 3.4.3.

$$\widehat{\mathcal{K}}_{h,i} = \{\widehat{K} := \otimes_{\alpha=1}^{d} (\zeta_j^\alpha, \zeta_{j+1}^\alpha),\ 1 \leqslant j \leqslant r_\alpha - 1\}_{t=1}^{n_i} .$$

For each $\widehat{K} \in \widehat{\mathcal{K}}_{h,i}$, let $\widehat{h}_{\widehat{K}}$ denote its diameter and $\widehat{h}_i := \max\{\widehat{h}_{\widehat{K}}\}$ denote the mesh-size of $\widehat{\mathcal{K}}_{h,i}$. The following are assumed:

1. quasi-uniformity: for every $\widehat{K} \in \widehat{\mathcal{K}}_{h,i}$, it holds that, $\widehat{h}_i \sim \widehat{h}_{\widehat{K}}$, i.e., there exist positive constants a, b, such that, $a\widehat{h}_i \leqslant \widehat{h}_{\widehat{K}} \leqslant b\widehat{h}_i$.

2. for the mesh element edges $e_{\widehat{K}} \subset \partial\widehat{K}$, $\widehat{h}_{\widehat{K}} \sim e_{\widehat{K}}$.

For each multi-index $\mathbf{j} := (j_1, \ldots, j_d)$ in the set $\mathcal{J} := \{\mathbf{j} = (j_1, \ldots, j_d) : 0 \leqslant j_\alpha \leqslant n_\alpha, \text{ for } 1 \leqslant \alpha \leqslant d\}$, the multivariate B-spline functions are given by

$$\widehat{N}_{\mathbf{j}}^{(i)} : \widehat{\Omega} \to \mathbb{R}, \quad \widehat{N}_{\mathbf{j}}^{(i)}(\boldsymbol{\eta}) := \prod_{\alpha=1}^{d} \widehat{N}_{j_\alpha}(\eta_\alpha)\,, \tag{4.1}$$

with the corresponding B-spline function space

$$\widehat{\mathcal{S}}_{h,i} := span\{\widehat{N}_{\mathbf{j}}^{(i)}\}_{\mathbf{j}\in\mathcal{J}}\,. \tag{4.2}$$

To obtain the NURBS functions on $\widehat{\Omega}$, the weighting functions are defined as

$$W^{(i)} : \widehat{\Omega} \longrightarrow \mathbb{R}, \quad W^{(i)}(\boldsymbol{\eta}) := \sum_{\mathbf{j}\in\mathcal{J}} \omega_{\mathbf{j}} \widehat{N}_{\mathbf{j}}^{(i)}(\boldsymbol{\eta}),$$

with the multivariate NURBS given by

$$\widehat{R}_{\mathbf{j}} : \widehat{\Omega} \longrightarrow \mathbb{R}, \quad \widehat{R}_{\mathbf{j}}(\boldsymbol{\eta}) = \frac{\widehat{N}_{\mathbf{j}}^{(i)}(\boldsymbol{\eta})\omega_{\mathbf{j}}}{W^{(i)}(\boldsymbol{\eta})}, \quad \forall \mathbf{j} \in \mathcal{J}, \tag{4.3}$$

with the corresponding NURBS space

$$\widehat{V}_{h,i} := span\{\widehat{R}_{\mathbf{j}}\}_{\mathbf{j}\in\mathcal{J}}\,.$$

For the set of control points $\{\mathbf{B}_{\mathbf{j}}^{(i)}\}_{\mathbf{j}\in\mathcal{J}} \subset \mathbb{R}^d$, each sub-domain $\Omega_i \in \mathcal{T}_h$, is exactly represented through the following geometrical mapping from $\widehat{\Omega}$ (parametric domain) to Ω_i (physical domain)

$$\Phi_i : \widehat{\Omega} \longrightarrow \Omega_i \subset \mathbb{R}^d, \quad \Phi_i(\boldsymbol{\eta}) = \sum_{\mathbf{j}\in\mathcal{J}} \widehat{R}_{\mathbf{j}}^{(i)}(\boldsymbol{\eta})\mathbf{B}_{\mathbf{j}}^{(i)} := \mathbf{x} \in \Omega_i, \tag{4.4}$$

where $\boldsymbol{\eta} := \Phi_i^{-1}(\mathbf{x})$.

Using Φ_i, the physical mesh $\mathcal{K}_{h,i} := \{K = \Phi_i(\widehat{K}),\ \widehat{K} \in \widehat{\mathcal{K}}_{h,i}\}$ can be constructed for every Ω_i.

Let h_K denote the diameter of K. If $h_i = \max\{h_K : K \in \mathcal{K}_{h,i}\}$ is the mesh size of sub-domain Ω_i, then by definition of the geometrical mapping given in (4.4), we have the equivalence relation $\widehat{h}_i \sim h_i$.

The mesh of Ω is taken to be

$$\mathcal{K}_h(\Omega) = \bigcup_{i=1}^{N} \mathcal{K}_{h,i}\,.$$

For the case of matching meshes, $h = h_i$, with h_i being constant for $i \in \{1, \ldots, N\}$.

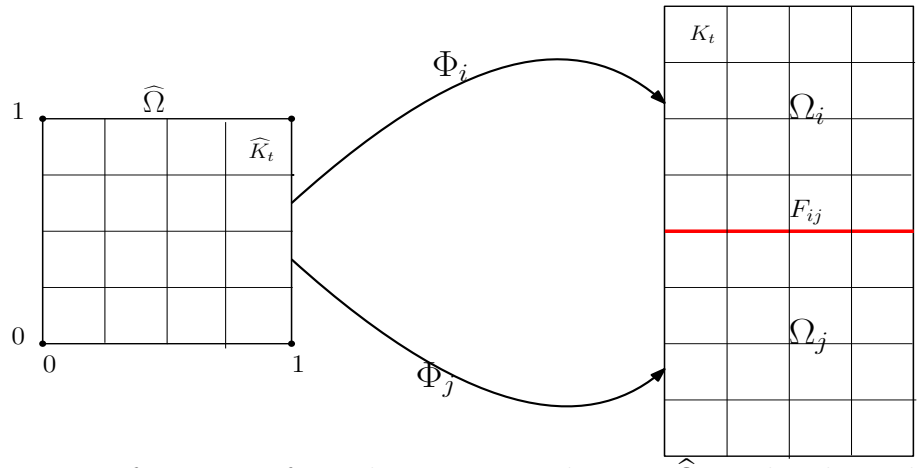

Figure 4.2: Transformations from the parameter domain, $\widehat{\Omega}$, to the physical domain, Ω, with $\Phi_i(\widehat{\Omega}) = \Omega_i$.

Next, using the "push-forward", Φ_i^{-1}, the B-spline space on Ω is given by

$$\mathcal{S}_h(\mathcal{T}_h) := \mathcal{S}_{h,1} \times \cdots \times \mathcal{S}_{h,N}, \tag{4.5}$$

$$\text{with, } \mathcal{S}_{h,i} := \left\{ N_{\mathbf{j}}^{(i)}\Big|_{\Omega_i} : N_{\mathbf{j}}^{(i)}(\boldsymbol{\eta}) = \widehat{N}_{\mathbf{j}}^{(i)} \circ \Phi_i^{-1}(\mathbf{x}), \quad \forall \widehat{N}_{\mathbf{j}}^{(i)} \in \widehat{\mathcal{S}}_{h,i} \right\}.$$

The NURBS space on Ω is similarly defined as

$$V_h(\mathcal{T}_h) := V_{h,1} \times \cdots \times V_{h,N} \tag{4.6}$$

$$\text{with, } V_{h,i} := \{\mathcal{R}_{\mathbf{j}}|_{\Omega_i} : \mathcal{R}_{\mathbf{j}}(\boldsymbol{\eta}) = \widehat{R}_{\mathbf{j}} \circ \Phi_i^{-1}(\mathbf{x}), \quad \forall R_{\mathbf{j}} \in \widehat{V}_{h,i}\}.$$

The B-spline space $\mathcal{S}_{h,i}$ or NURBS space $V_{h,i}$ are used for approximating the solution to the weak form (3.34) in every sub-domain Ω_i.

For a function $v \in H^1(\Omega, \mathcal{T}_h)$, and $F \in \mathcal{F}$, let $v_i = v|_{\partial\Omega_i \bigcap F}$ and $v_j = v|_{\partial\Omega_j \bigcap F}$, then the jumps and averages are defined as

$$\text{Average: } \{v\} := \frac{1}{2}(v_i + v_j); \quad \text{Jump: } [v] := v_i - v_j, \quad \text{for } F_{ij} \in \mathcal{F}_I\,, \tag{4.7}$$

$$\text{Average: } \{v\} := v_i; \quad \text{Jump: } [v] := v_i, \quad \text{for } F_i \in \mathcal{F}_D. \tag{4.8}$$

For what follows, depending on the context, $\mathbf{n} = \mathbf{n}_i$ is taken to be the external unit normal vector associated with each $F_i \in \mathcal{F}_D$ or the unit normal vector directed from Ω_i to Ω_j, associated with each interface $F_{ij} \in \mathcal{F}_I$.

4.3 Interior Penalty Variational Formulation

Here, for simplicity, the Dirichlet version of problem (3.30) is considered, that is: Find $u : \overline{\Omega} \to \mathbb{R}$, such that

$$\Delta^2 u = f \quad \text{in } \Omega, \tag{4.9}$$

$$u = g_0 \quad \text{on } \partial\Omega, \tag{4.10}$$

$$\mathbf{n} \cdot \nabla u = g_1 \quad \text{on } \partial\Omega. \tag{4.11}$$

Multiplying the model problem (4.9) by a test function v and integrating by parts twice over each sub-domain $\Omega_i,\ i = 1, \ldots, N$, gives for $u \in H^4(\Omega_i)$,

$$\int_{\Omega_i} f v \mathrm{d}\Omega = \int_{\Omega_i} \Delta u \Delta v \mathrm{d}\Omega - \int_{\partial\Omega_i} (\mathbf{n} \cdot \nabla v) \Delta u \mathrm{d}\Gamma + \int_{\partial\Omega_i} (\mathbf{n} \cdot \nabla \Delta u) v \mathrm{d}\Gamma, \quad \forall v \in H^2(\Omega_i). \tag{4.12}$$

Summing (4.12) over all sub-domains gives

$$\sum_{i=1}^{N} \int_{\Omega_i} f v \mathrm{d}\Omega = \sum_{i=1}^{N} \int_{\Omega_i} \Delta u \Delta v \mathrm{d}\Omega - \sum_{i=1}^{N} \int_{\partial\Omega_i} (\mathbf{n} \cdot \nabla v) \Delta u \mathrm{d}\Gamma + \sum_{i=1}^{N} \int_{\partial\Omega_i} (\mathbf{n} \cdot \nabla \Delta u) v \mathrm{d}\Gamma. \tag{4.13}$$

The sum of the boundary integrals are rewritten as follows

$$\sum_{i=1}^{N}\int_{\partial\Omega_i}(\mathbf{n}\cdot\nabla v)\Delta u\mathrm{d}\Gamma = \sum_{F_{ij}\in\mathcal{F}_I}\int_{F_{ij}}\mathbf{n}\cdot(\nabla v_i\Delta u_i - \nabla v_j\Delta u_j)\mathrm{d}\Gamma + \sum_{F_i\in\mathcal{F}_D}\int_{F_i}(\mathbf{n}\cdot\nabla v_i)\Delta u_i\mathrm{d}\Gamma, \tag{4.14}$$

and

$$\sum_{i=1}^{N}\int_{\partial\Omega_i}(\mathbf{n}\cdot\nabla\Delta u)v\mathrm{d}\Gamma = \sum_{F_{ij}\in\mathcal{F}_I}\int_{F_{ij}}\mathbf{n}\cdot(\nabla\Delta u_i)v_i - \mathbf{n}\cdot(\nabla\Delta u_j)v_j\mathrm{d}\Gamma + \sum_{F_i\in\mathcal{F}_D}\int_{F_i}(\mathbf{n}\cdot\nabla\Delta u_i)v_i\mathrm{d}\Gamma. \tag{4.15}$$

Substituting (4.14) and (4.15) into (4.13) yields

$$\sum_{i=1}^{N}\int_{\Omega_i}fv\mathrm{d}\Omega = \sum_{i=1}^{N}\int_{\Omega_i}\Delta u\Delta v\mathrm{d}\Omega - \sum_{F\in\mathcal{F}}\int_{F}[\mathbf{n}\cdot\nabla v\Delta u]\mathrm{d}\Gamma + \sum_{F\in\mathcal{F}}\int_{F}[(\mathbf{n}\cdot\nabla\Delta u)v]\mathrm{d}\Gamma, \tag{4.16}$$

where $F\in\mathcal{F}$ means $F_{ij}\in\mathcal{F}_I$, or $F_i\in\mathcal{F}_D$.

For the fluxes at each interface $F_{ij}\in\mathcal{F}_I$, using the definitions of the jumps and averages (4.8), we have the following relation

$$\begin{aligned}[\mathbf{n}\cdot\nabla v\Delta u] &= \mathbf{n}\cdot(\nabla v_i\Delta u_i - \nabla v_j\Delta u_j)\\ &= \frac{1}{2}(\mathbf{n}\cdot\nabla v_i)\Delta u_i + \frac{1}{2}(\mathbf{n}\cdot\nabla v_j)\Delta u_i - \frac{1}{2}(\mathbf{n}\cdot\nabla v_i)\Delta u_j - \frac{1}{2}(\mathbf{n}\cdot\nabla v_j)\Delta u_j\\ &+ \frac{1}{2}(\mathbf{n}\cdot\nabla v_i)\Delta u_i + \frac{1}{2}(\mathbf{n}\cdot\nabla v_i)\Delta u_j - \frac{1}{2}(\mathbf{n}\cdot\nabla v_j)\Delta u_i - \frac{1}{2}(\mathbf{n}\cdot\nabla v_j)\Delta u_j\\ &= \frac{1}{2}(\mathbf{n}\cdot\nabla v_i)(\Delta u_i - \Delta u_j) + \frac{1}{2}(\mathbf{n}\cdot\nabla v_j)(\Delta u_i - \Delta u_j)\end{aligned}$$

$$+\frac{1}{2}(\mathbf{n}\cdot\nabla v_i)(\Delta u_i+\Delta u_j)-\frac{1}{2}(\mathbf{n}\cdot\nabla v_j)(\Delta u_i+\Delta u_j)$$
$$=\{\mathbf{n}\cdot\nabla v\}[\Delta u]+\{\Delta u\}[\mathbf{n}\cdot\nabla v]. \tag{4.17}$$

By the regularity of the solution u, it follows that $\Delta u|_{\partial\Omega_i}\in H^{\frac{3}{2}}(\partial\Omega_i)$ by an extension of Theorem 3.2.2, thus, $[\Delta u]=0$. Therefore

$$[\mathbf{n}\cdot\nabla v\Delta u]=[\mathbf{n}\cdot\nabla v]\{\Delta u\}. \tag{4.18}$$

By using the regularity of the solution, and since $\nabla\Delta u|_{\partial\Omega_i}\in H^{\frac{1}{2}}(\partial\Omega_i)$, it follows that

$$[(\mathbf{n}\cdot\nabla\Delta u)v]=\{\mathbf{n}\cdot\nabla\Delta u\}[v]+[\mathbf{n}\cdot\nabla\Delta u]\{v\}=\{\mathbf{n}\cdot\nabla\Delta u\}[v]. \tag{4.19}$$

Using the relations (4.18) and (4.19),

$$\sum_{F\in\mathcal{F}}\int_F[\mathbf{n}\cdot\nabla v\Delta u]\mathrm{d}\Gamma=\sum_{F\in\mathcal{F}}\int_F\{\Delta u\}[\mathbf{n}\cdot\nabla v]\mathrm{d}\Gamma, \tag{4.20}$$

and

$$\sum_{F\in\mathcal{F}}\int_F[(\mathbf{n}\cdot\nabla\Delta u)v]\mathrm{d}\Gamma=\sum_{F\in\mathcal{F}}\int_F\{\mathbf{n}\cdot\nabla\Delta u\}[v]\mathrm{d}\Gamma. \tag{4.21}$$

Putting (4.20) and (4.21) into (4.16) gives

$$\sum_{i=1}^{N}\int_{\Omega_i}fv\mathrm{d}\Omega=\sum_{i=1}^{N}\int_{\Omega_i}\Delta u\Delta v\mathrm{d}\Omega-\sum_{F\in\mathcal{F}}\int_F\{\Delta u\}[\mathbf{n}\cdot\nabla v]\mathrm{d}\Gamma$$
$$+\sum_{F\in\mathcal{F}}\int_F\{\mathbf{n}\cdot\nabla\Delta u\}[v]\mathrm{d}\Gamma. \tag{4.22}$$

Due to the regularity of the solution u, both the jump of the solution and the jump of the fluxes of the solution are zero, i.e., $[u]=0$ and $[\mathbf{n}\cdot\nabla u]=0$. The following consistency terms can be added to (4.22).

$$\beta_1\sum_{F\in\mathcal{F}}\int_F\{\Delta v\}[\mathbf{n}\cdot\nabla u]\mathrm{d}\Gamma+\beta_2\sum_{F\in\mathcal{F}}\int_F\{\mathbf{n}\cdot\nabla\Delta v\}[u]\mathrm{d}\Gamma. \tag{4.23}$$

Where

$$\sum_{F\in\mathcal{F}}\int_F \{\Delta v\}[\mathbf{n}\cdot\nabla u]\mathrm{d}\Gamma = \sum_{F_{ij}\in\mathcal{F}_I}\int_{F_{ij}} \{\Delta v\}[\mathbf{n}\cdot\nabla u]\mathrm{d}\Gamma + \sum_{F_i\in\mathcal{F}_D}\int_{F_i} \{\Delta v\}[\mathbf{n}\cdot\nabla u - g_1]\mathrm{d}\Gamma,$$

and

$$\sum_{F\in\mathcal{F}}\int_F \{\mathbf{n}\cdot\nabla\Delta v\}[u]\mathrm{d}\Gamma = \sum_{F_{ij}\in\mathcal{F}_I}\int_{F_{ij}} \{\mathbf{n}\cdot\nabla\Delta v\}[u]\mathrm{d}\Gamma + \sum_{F_i\in\mathcal{F}_D}\int_{F_i} \{\mathbf{n}\cdot\nabla\Delta v\}[u - g_0]\mathrm{d}\Gamma,$$

and $\beta_1, \beta_2 \in [-1, 1]$.

The following consistency terms are added to penalize the jumps of the solution and the jumps of the fluxes of the solution

$$J_0(u,v) = \sum_{F_{ij}\in\mathcal{F}_I}\frac{\sigma_0}{h_i^3}\int_{F_{ij}}[u][v]\mathrm{d}\Gamma + \sum_{F_i\in\mathcal{F}_D}\frac{\sigma_0}{h_i^3}\int_{F_i}(u-g_0)v\mathrm{d}\Gamma, \tag{4.24}$$

$$J_1(u,v) = \sum_{F_{ij}\in\mathcal{F}_I}\frac{\sigma_1}{h_i}\int_{F_{ij}}[\mathbf{n}\cdot\nabla u][\mathbf{n}\cdot\nabla v]\mathrm{d}\Gamma + \sum_{F_i\in\mathcal{F}_D}\frac{\sigma_1}{h_i}\int_{F_i}(\mathbf{n}\cdot\nabla u - g_1)(\mathbf{n}\cdot\nabla v)\,\mathrm{d}\Gamma, \tag{4.25}$$

where σ_0, σ_1 are positive constants called penalty parameters.

Finally, the interior penalty variational scheme reads: Find $u \in H^4(\Omega, \mathcal{T}_h)$ such that,

$$a_h(u,v) = L(v), \quad \forall v \in H^4(\Omega, \mathcal{T}_h), \tag{4.26}$$

where the bilinear form is given by

$$a_h(u,v) = \sum_{i=1}^{N}\int_{\Omega_i}\Delta u\Delta v\mathrm{d}\Omega - \sum_{F\in\mathcal{F}}\int_F\{\Delta u\}[\mathbf{n}\cdot\nabla v]\mathrm{d}\Gamma + \beta_1\sum_{F\in\mathcal{F}}\int_F\{\Delta v\}[\mathbf{n}\cdot\nabla u]\mathrm{d}\Gamma$$

$$+ \sum_{F\in\mathcal{F}} \int_F \{\mathbf{n}\cdot\nabla\Delta u\}[v]\mathrm{d}\Gamma + \beta_2 \sum_{F\in\mathcal{F}} \int_F \{\mathbf{n}\cdot\nabla\Delta v\}[u]\mathrm{d}\Gamma$$

$$+ \sum_{F\in\mathcal{F}} \frac{\sigma_0}{h_i^3} \int_F [u][v]\mathrm{d}\Gamma + \sum_{F\in\mathcal{F}} \frac{\sigma_1}{h_i} \int_F [\mathbf{n}\cdot\nabla u][\mathbf{n}\cdot\nabla v]\mathrm{d}\Gamma, \tag{4.27}$$

and the linear form is given as

$$L(v) = \sum_{i=1}^{N} \int_{\Omega_i} f v \mathrm{d}\Omega + \sum_{F_i\in\mathcal{F}_D} \int_{F_i} \left(\frac{\sigma_0}{h_i^3} v_h + \beta_2 \mathbf{n}\cdot\nabla\Delta v_h \right) g_0 \mathrm{d}\Gamma$$

$$+ \sum_{F_i\in\mathcal{F}_D} \int_{F_i} \left(\frac{\sigma_1}{h_i} (\mathbf{n}\cdot\nabla v_h) + \beta_1 \Delta v_h \right) g_1 \mathrm{d}\Gamma. \tag{4.28}$$

The choice of β_1 and β_2 yields different schemes.

1. Taking $\beta_1 = \beta_2 = -1$ gives the Semi-Symmetric Interior Penalty Galerkin 1 (SSIPG1) scheme.

2. Taking $\beta_1 = \beta_2 = +1$ gives the Semi-Symmetric Interior Penalty Galerkin 2 (SSIPG2) scheme.

3. Taking $\beta_1 = -1$, $\beta_2 = +1$ gives the Symmetric Interior Penalty Galerkin (SIPG) scheme.

4. Taking $\beta_1 = +1$, $\beta_2 = -1$ gives the Non-symmetric Interior Penalty Galerkin (NIPG) scheme.

The analysis in this thesis is restricted to the SIPG scheme.

4.4 dG-IgA Approximation

Let $V_h \subset H^4(\Omega, \mathcal{T}_h)$, be the finite dimensional NURBS subspace. Then, the dG-IgA scheme reads: find $u_h \in V_h$ such that

$$a_h(u_h, v_h) = L(v_h), \quad \forall v_h \in V_h, \tag{4.29}$$

where the bilinear form is given by

$$
\begin{aligned}
a_h(u_h, v_h) = &\sum_{i=1}^{N} \int_{\Omega_i} \Delta u_h \Delta v_h \mathrm{d}\Omega \\
&- \sum_{F\in\mathcal{F}} \int_F [\mathbf{n}\cdot\nabla v_h]\{\Delta u_h\}\mathrm{d}\Gamma - \sum_{F\in\mathcal{F}} \int_F [\mathbf{n}\cdot\nabla u_h]\{\Delta v_h\}\mathrm{d}\Gamma \\
&+ \sum_{F\in\mathcal{F}} \int_F \{\mathbf{n}\cdot\nabla\Delta u_h\}[v_h]\mathrm{d}\Gamma + \sum_{F\in\mathcal{F}} \int_F \{\mathbf{n}\cdot\nabla\Delta v_h\}[u_h]\mathrm{d}\Gamma \\
&+ \sum_{F\in\mathcal{F}} \frac{\sigma_0}{h_i^3} \int_F [u_h][v_h]\mathrm{d}\Gamma + \sum_{F\in\mathcal{F}} \frac{\sigma_1}{h_i} \int_F [\mathbf{n}\cdot\nabla u_h][\mathbf{n}\cdot\nabla v_h]\mathrm{d}\Gamma, \qquad (4.30)
\end{aligned}
$$

and the linear form is given as

$$
\begin{aligned}
L(v_h) = &\sum_{i=1}^{N} \int_{\Omega_i} f v_h \mathrm{d}\Omega + \sum_{F_i\in\mathcal{F}_D} \int_{F_i} \left(\frac{\sigma_0}{h_i^3} v_h + \mathbf{n}\cdot\nabla\Delta v_h\right) g_0 \mathrm{d}\Gamma \\
&+ \sum_{F_i\in\mathcal{F}_D} \int_{F_i} \left(\frac{\sigma_1}{h_i}(\mathbf{n}\cdot\nabla v_h) - \Delta v_h\right) g_1 \mathrm{d}\Gamma. \qquad (4.31)
\end{aligned}
$$

Next, the following discrete norm is defined.

$$
\|v\|_h^2 = \sum_{i=1}^{N} \|\Delta v\|_{L^2(\Omega_i)}^2 + \sum_{F\in\mathcal{F}} \frac{\sigma_0}{h_i^3} \|[v]\|_{L^2(F)}^2 + \sum_{F\in\mathcal{F}} \frac{\sigma_1}{h_i} \|[\mathbf{n}\cdot\nabla v]\|_{L^2(F)}^2, \quad v \in H^2(\Omega, \mathcal{T}_h). \qquad (4.32)
$$

Proposition 4.4.1. (4.32) *is a norm on* $H^2(\Omega, \mathcal{T}_h)$.

Proof. For some $v \in H^2(\Omega, \mathcal{T}_h)$, $\|\Delta v\|_{L^2(\Omega_i)} \geqslant 0$, for $i = 1, \ldots, N$.

$$
\|[v]\|_{L^2(F)}^2 \geqslant 0, \quad \text{and} \quad \|[\mathbf{n}\cdot\nabla v]\|_{L^2(F)}^2 \geqslant 0, \quad \forall F \in \mathcal{F}.
$$

Thus, $\|v\|_h \geqslant 0, \quad \forall v \in H^2(\Omega, \mathcal{T}_h)$.

If $\|v\|_h = 0$, then $\Delta v = 0$ in $\Omega_i, \quad \forall i = 1, \ldots, N$, and the jumps $[v]$ and $[\mathbf{n}\cdot\nabla v]$ are zero on the interfaces $F_{ij} \in \mathcal{F}_I$. Also, for $\|v\|_h = 0$, it means $v_i = 0$ and $\mathbf{n}\cdot\nabla v_i = 0$ on $F_i \in \mathcal{F}_D$. Thus, $v = 0$ on the whole domain $\overline{\Omega}$. The rest of the axioms can be proven. □

4.5 Some Properties

In this section, some of the properties of the bilinear form obtained for the dG-IgA scheme for the problem (4.9) are shown. In the following theorem, it is shown that, the discontinuous weak formulation of problem (4.9) is consistent with the usual variational formulation of the problem, and thus consistent with the strong form of the problem.

Theorem 4.5.1 (Consistency)**.** *Assume that the weak solution u of problem* (4.9)-(4.11) *belongs to $H^4(\Omega, \mathcal{T}_h)$, then u satisfies the variational problem* (4.26)*. Conversely, if $u \in H^4(\Omega) \bigcap H^4(\Omega, \mathcal{T}_h)$, satisfies* (4.26)*, then u is the solution to problem* (4.9)-(4.11)*.*

Proof. The first part follows from the derivation in section 4.3. For the converse, first take $v \in C_0^\infty(\Omega_i)$, then (4.26) reduces to

$$\sum_{i=1}^{N} \int_{\Omega_i} f v \mathrm{d}\Omega = \sum_{i=1}^{N} \int_{\Omega_i} \Delta u \Delta v \mathrm{d}\Omega.$$

Which yields in the distributional sense, for all $\Omega_i \in \mathcal{T}_h$,

$$\Delta^2 u = f, \quad \text{in } \Omega_i. \tag{4.33}$$

Next, let F_{12} be the interface between two adjacent sub-domains Ω_1 and Ω_2, and take $v \in H_0^4(\Omega_1 \bigcup \Omega_2)$, extending it by zero over the rest of Ω. Then, multiplying through (4.33) by such v and integrating by parts twice gives

$$\int_{\Omega_1 \bigcup \Omega_2} f v \mathrm{d}\Omega = \int_{\Omega_1 \bigcup \Omega_2} \Delta u \Delta v \mathrm{d}\Omega - \int_{F_{12}} \mathbf{n} \cdot \nabla v [\Delta u] \mathrm{d}\Gamma + \int_{F_{12}} [\mathbf{n} \cdot \nabla \Delta u] v \mathrm{d}\Gamma.$$

On the other hand, for $v \in H_0^4(\Omega_1 \bigcup \Omega_2)$, (4.26) reduces to

$$\int_{\Omega_1 \bigcup \Omega_2} f v \mathrm{d}\Omega = \int_{\Omega_1 \bigcup \Omega_2} \Delta u \Delta v \mathrm{d}\Omega.$$

Thus, $\forall v \in H_0^4(\Omega_1 \bigcup \Omega_2)$,

$$\int_{F_{12}} \mathbf{n} \cdot \nabla v [\Delta u] \mathrm{d}\Gamma = \int_{F_{12}} [\mathbf{n} \cdot \nabla \Delta u] v \mathrm{d}\Gamma.$$

But this is only possible if $[\Delta u]|_{F_{12}} = 0$, and $[\mathbf{n} \cdot \nabla \Delta u]|_{F_{12}} = 0$ in $L^2(F_{12})$. Since this holds over all $F \in \mathcal{F}$, it implies that $\Delta^2 u \in L^2(\Omega)$. Hence globally,

$$\Delta^2 u = f \quad \text{in } \Omega. \tag{4.34}$$

Next, let $v \in H^4(\Omega) \bigcap H_0^2(\Omega)$, then multiplying through (4.34) by such v and integrating by parts twice gives

$$\sum_{i=1}^{N} \int_{\Omega_i} f v \mathrm{d}\Omega = \sum_{i=1}^{N} \int_{\Omega_i} \Delta u \Delta v \mathrm{d}\Omega.$$

On the other hand, for $v \in H^4(\Omega) \bigcap H_0^2(\Omega)$, (4.26) reduces to

$$\sum_{i=1}^{N} \int_{\Omega_i} f v \mathrm{d}\Omega = \sum_{i=1}^{N} \int_{\Omega_i} \Delta u \Delta v \mathrm{d}\Omega - \sum_{F_i \in \mathcal{F}_D} \int_{F_i} \Delta v (\mathbf{n} \cdot \nabla u - g_1) \mathrm{d}\Gamma$$
$$+ \sum_{F_i \in \mathcal{F}_D} \int_{F_i} (\mathbf{n} \cdot \nabla \Delta v)(u - g_0) \mathrm{d}\Gamma.$$

Comparing the two, it can be concluded that, for each $F_i \in \mathcal{F}_D$,

$$\int_{F_i} \Delta v (\mathbf{n} \cdot \nabla u - g_1) \mathrm{d}\Gamma = \int_{F_i} (\mathbf{n} \cdot \nabla \Delta v)(u - g_0) \mathrm{d}\Gamma.$$

But since v is arbitrary, this is only possible if

$$(u - g_0)|_{F_i} = 0, \quad \text{and } (\mathbf{n} \cdot \nabla u - g_1)|_{F_i} = 0.$$

Thus

$$u = g_0 \text{ on } F_i = \partial\Omega_i \bigcap \partial\Omega,$$

$$\mathbf{n} \cdot \nabla u = g_1 \text{ on } F_i = \partial\Omega_i \bigcap \partial\Omega,$$

which are the Dirichlet boundary conditions of problem (4.9)-(4.11). □

In order to present subsequent results, including the coercivity and boundedness properties of the bilinear form, the following lemmata are required.
The scaled trace inequality for a patch is given by the following lemma.

Lemma 4.5.2. *Let $K \in \mathcal{K}_{h,i}$, $i = 1, \ldots, N$ and $\widehat{K} = \Phi_i^{-1}(K)$. Then the scaled trace inequality*

$$\|v\|_{L^2(\partial\Omega_i)} \leqslant C_{tr,u} h_i^{-1/2} \left(\|v\|_{L^2(\Omega_i)} + h_i |v|_{H^1(\Omega_i)} \right), \tag{4.35}$$

holds for all $v \in H^1(\Omega_i)$, where h_i denotes the global mesh size of patch Ω_i in the physical domain, and $C_{tr,u}$ is a positive constant that only depends on the quasi-uniformity and shape regularity of the mapping Φ_i.

Proof. See [Chapter 2 in Moore (2017)]. □

Lemma 4.5.3. *Let $K \in \mathcal{K}_{h,i}$, where $\mathcal{K}_{h,i}$ is the underlying mesh of Ω_i. Then the inverse inequalities*

$$\|v_h\|_{L^2(\partial\Omega_i)} \leqslant C_{inv,0,u} h_i^{-1/2} \|v_h\|_{L^2(\Omega_i)}, \tag{4.36}$$

$$\|\nabla v_h\|_{L^2(\Omega_i)} \leqslant C_{inv,1,u} h_i^{-1} \|v_h\|_{L^2(\Omega_i)}, \tag{4.37}$$

hold for all $v_h \in V_h$, where $C_{inv,1,u}$ and $C_{inv,0,u}$ are positive constants, which are independent of h_i and $\Omega_i \in \mathcal{T}_h$.

Proof. See [Moore (2017)]. □

Proposition 4.5.4. *Let $K \in \mathcal{K}_{h,i}$, where $\mathcal{K}_{h,i}$ is the underlying mesh of Ω_i. Then the inverse inequality*

$$\|\nabla v_h\|_{L^2(\partial\Omega_i)} \leqslant C_{inv,0,1,u} h_i^{-\frac{3}{2}} \|v_h\|_{L^2(\Omega_i)}, \tag{4.38}$$

holds for all $v_h \in V_h$, where $C_{inv,0,1,u} = C_{inv,1,u} C_{inv,0,u}$ and $C_{inv,1,u}$ and $C_{inv,0,u}$ are as stated in lemma 4.5.3.

Proof. By using the inequalities (4.36) and (4.37) of Lemma 4.5.3,

$$\begin{aligned}\|\nabla v_h\|_{L^2(\partial\Omega_i)} &\leqslant C_{inv,0,u} h_i^{-1/2} \|\nabla v_h\|_{L^2(\Omega_i)}, \\ &\leqslant C_{inv,0,u} C_{inv,1,u} h_i^{-\frac{1}{2}} h_i^{-1} \|v_h\|_{L^2(\Omega_i)}, \\ &= C_{inv,0,1,u} h_i^{-\frac{3}{2}} \|v_h\|_{L^2(\Omega_i)}.\end{aligned}$$

□

The next lemma is required to prove for the coercivity of the bilinear form.

Lemma 4.5.5. *Let ε be a positive constant and $F \in \mathcal{F}$, then the estimates*

$$\left| \int_F \{\mathbf{n} \cdot \nabla \Delta v_h\} [v_h] \, d\Gamma \right| \leqslant \varepsilon \frac{C_{inv,0,1,u}}{2\sigma_0} \|\Delta v_h\|^2_{L^2(\Omega_i)} + \frac{\alpha}{2\varepsilon} \|[v_h]\|^2_{L^2(F)}, \tag{4.39}$$

$$\left| \int_F \{\Delta v_h\} [\mathbf{n} \cdot \nabla v_h] \, d\Gamma \right| \leqslant \varepsilon \frac{C_{inv,0,u}}{2\sigma_1} \|\Delta v_h\|^2_{L^2(\Omega_i)} + \frac{\beta}{2\varepsilon} \|[\mathbf{n} \cdot \nabla v_h]\|^2_{L^2(F)}, \tag{4.40}$$

hold for all $v_h \in V_h$, with $\alpha := \frac{\sigma_0}{h_i^3}$, and $\beta := \frac{\sigma_1}{h_i}$ and where $C_{inv,0,1,u}$ and $C_{inv,0,u}$ are independent of the mesh size h_i, but dependent on the NURBS degree p.

Proof. For (4.39), applying the Cauchy-Schwarz inequality and subsequently, Young's inequality,

$$\begin{aligned}\left| \int_F \{\mathbf{n} \cdot \nabla \Delta v_h\} [v_h] \mathrm{d}\Gamma \right| &= \left| \int_F \frac{1}{\sqrt{\alpha}} \{\mathbf{n} \cdot \nabla \Delta v_h\} \sqrt{\alpha} [v_h] \mathrm{d}\Gamma \right| \\ &\leqslant \left(\int_F \frac{1}{\alpha} |\{\mathbf{n} \cdot \nabla \Delta v_h\}|^2 \mathrm{d}\Gamma \right)^{\frac{1}{2}} \left(\int_F \alpha |[v_h]|^2 \mathrm{d}\Gamma \right)^{\frac{1}{2}} \\ &\leqslant \frac{\varepsilon}{2} \left(\int_F \frac{1}{\alpha} |\{\mathbf{n} \cdot \nabla \Delta v_h\}|^2 \mathrm{d}\Gamma \right) + \frac{1}{2\varepsilon} \left(\int_F \alpha |[v_h]|^2 \mathrm{d}\Gamma \right) \\ &= \frac{\varepsilon}{2} \| \frac{1}{\sqrt{\alpha}} \{\mathbf{n} \cdot \nabla \Delta v_h\} \|^2_{L^2(F)} + \frac{\alpha}{2\varepsilon} \|[v_h]\|^2_{L^2(F)}. \end{aligned} \tag{4.41}$$

Using (4.38), the first part of the right-hand-side of (4.41) is estimated as follows

$$\frac{\varepsilon}{2} \| \frac{1}{\sqrt{\alpha}} \{\mathbf{n} \cdot \nabla \Delta v_h\} \|^2_{L^2(F)} = \frac{\varepsilon}{2\alpha} \| \frac{1}{2} \left(\mathbf{n} \cdot \nabla \Delta v_{h,i} + \mathbf{n} \cdot \nabla \Delta v_{h,j} \right) \|^2_{L^2(F)}$$

$$
\begin{aligned}
&\leqslant \frac{\varepsilon}{4\alpha}\left(\|\nabla\Delta v_{h,i}\|^2_{L^2(F)} + \|\nabla\Delta v_{h,j}\|^2_{L^2(F)}\right)\\
&= 2\frac{\varepsilon}{4\alpha}\|\nabla\Delta v_{h,i}\|^2_{L^2(\partial\Omega_i\setminus(\partial\Omega_i\bigcap\partial\Omega))}\\
&\leqslant \frac{\varepsilon}{2\alpha}\|\nabla\Delta v_{h,i}\|^2_{L^2(\partial\Omega_i)}\\
&\leqslant \varepsilon\frac{C_{inv,0,1,u}}{2\alpha h_i^3}\|\Delta v_{h,i}\|^2_{L^2(\Omega_i)} = \varepsilon\frac{C_{inv,0,1,u}}{2\sigma_0}\|\Delta v_h\|^2_{L^2(\Omega_i)}.
\end{aligned}
\tag{4.42}
$$

Substituting (4.42) into (4.41) gives (4.39).

For (4.40), following arguments similar to those used for (4.39),

$$
\begin{aligned}
\left|\int_F \{\Delta v_h\}[\mathbf{n}\cdot\nabla v_h]\mathrm{d}\Gamma\right| &= \left|\int_F \frac{1}{\sqrt{\beta}}\{\Delta v_h\}\sqrt{\beta}[\mathbf{n}\cdot\nabla v_h]\mathrm{d}\Gamma\right|\\
&\leqslant \left(\int_F \frac{1}{\beta}|\{\Delta v_h\}|^2\mathrm{d}\Gamma\right)^{\frac{1}{2}}\left(\int_F \beta|[\mathbf{n}\cdot\nabla v_h]|^2\mathrm{d}\Gamma\right)^{\frac{1}{2}}\\
&\leqslant \frac{\varepsilon}{2}\int_F \frac{1}{\beta}|\{\Delta v_h\}|^2\mathrm{d}\Gamma + \frac{1}{2\varepsilon}\int_F \beta|[\mathbf{n}\cdot\nabla v_h]|^2\mathrm{d}\Gamma\\
&= \frac{\varepsilon}{2}\|\frac{1}{\sqrt{\beta}}\{\Delta v_h\}\|^2_{L^2(F)} + \frac{\beta}{2\varepsilon}\|[\mathbf{n}\cdot\nabla v_h]\|^2_{L^2(F)}\,.
\end{aligned}
\tag{4.43}
$$

Using Lemma 4.5.3, the first part of the right-hand-side of (4.43) is estimated as follows

$$
\begin{aligned}
\frac{\varepsilon}{2}\|\frac{1}{\sqrt{\beta}}\{\Delta v_h\}\|^2_{L^2(F)} &= \frac{\varepsilon}{2\beta}\|\frac{1}{2}\left(\Delta v_{h,i} + \Delta v_{h,j}\right)\|^2_{L^2(F)}\\
&\leqslant \frac{\varepsilon}{4\beta}\left(\|\Delta v_{h,i}\|^2_{L^2(F)} + \|\Delta v_{h,j}\|^2_{L^2(F)}\right)\\
&= 2\frac{\varepsilon}{4\beta}\|\Delta v_{h,i}\|^2_{L^2(\partial\Omega_i\setminus(\partial\Omega_i\bigcap\partial\Omega))}\\
&\leqslant \frac{\varepsilon}{2\beta}\|\Delta v_{h,i}\|^2_{L^2(\partial\Omega_i)}\\
&\leqslant \varepsilon\frac{C_{inv,0,u}}{2\beta h_i}\|\Delta v_{h,i}\|^2_{L^2(\Omega_i)} = \varepsilon\frac{C_{inv,0,u}}{2\sigma_1}\|\Delta v_h\|^2_{L^2(\Omega_i)}.
\end{aligned}
\tag{4.44}
$$

Substituting (4.44) into (4.43) gives (4.40). □

Theorem 4.5.6 (Coercivity)**.** *Let $a_h(\cdot,\cdot)$ be the bilinear form defined in* (4.29)*, and let $C_{inv,0,1,u}, C_{inv,0,u} > 0$ be the constants from lemma 4.5.5. Choosing σ_0 and σ_1 such that $\sigma_0 \geqslant \underline{\sigma}_0$ and $\sigma_1 \geqslant \underline{\sigma}_1$ and $\frac{C_{inv,0,1,u}}{\underline{\sigma}_0} + \frac{C_{inv,0,u}}{\underline{\sigma}_1} < 1$ for $\underline{\sigma}_0, \underline{\sigma}_1 \geqslant 0$. Then there exist a constant $\mu_c > 0$ such that*

$$a_h(v_h, v_h) \geqslant \mu_c \|v_h\|_h^2, \quad \forall v_h \in V_h. \tag{4.45}$$

Proof. For arbitrary $v_h \in V_h$,

$$\begin{aligned}
a_h(v_h, v_h) &= \sum_{i=1}^{N} \int_{\Omega_i} (\Delta v_h)^2 \mathrm{d}\Omega - 2 \sum_{F\in\mathcal{F}} \int_F [\mathbf{n}\cdot\nabla v_h]\{\Delta v_h\}\mathrm{d}\Gamma \\
&\quad + 2 \sum_{F\in\mathcal{F}} \int_F \{\mathbf{n}\cdot\nabla\Delta v_h\}[v_h]\mathrm{d}\Gamma + \sum_{F\in\mathcal{F}} \int_F \frac{\sigma_0}{h_i^3}[v_h]^2\mathrm{d}\Gamma \\
&\quad + \sum_{F\in\mathcal{F}} \int_F \frac{\sigma_1}{h_i}[\mathbf{n}\cdot\nabla v_h]^2\mathrm{d}\Gamma \\
&= \sum_{i=1}^{N} \|\Delta v_h\|_{L^2(\Omega_i)}^2 + \sum_{F\in\mathcal{F}} \frac{\sigma_0}{h_i^3}\|[v_h]\|_{L^2(F)}^2 + \sum_{F\in\mathcal{F}} \int_F \frac{\sigma_1}{h_i}\|[\mathbf{n}\cdot\nabla v_h]\|_{L^2(F)}^2 \\
&\quad - 2 \sum_{F\in\mathcal{F}} \int_F [\mathbf{n}\cdot\nabla v_h]\{\Delta v_h\}\mathrm{d}\Gamma + 2 \sum_{F\in\mathcal{F}} \int_F \{\mathbf{n}\cdot\nabla\Delta v_h\}[v_h]\mathrm{d}\Gamma.
\end{aligned} \tag{4.46}$$

By using (4.39) and (4.40) of Lemma 4.5.5,

$$\sum_{F\in\mathcal{F}} \int_F \{\mathbf{n}\cdot\nabla\Delta v_h\}[v_h]\mathrm{d}\Gamma \leqslant \sum_{F\in\mathcal{F}} \left(\varepsilon \frac{C_{inv,0,1,u}}{2\sigma_0} \|\Delta v_h\|_{L^2(\Omega_i)}^2 + \frac{\alpha}{2\varepsilon} \|[v_h]\|_{L^2(F)}^2 \right), \tag{4.47}$$

and,

$$\sum_{F\in\mathcal{F}} \int_F [\mathbf{n}\cdot\nabla v_h]\{\Delta v_h\}\mathrm{d}\Gamma \leqslant \sum_{F\in\mathcal{F}} \left(\varepsilon \frac{C_{inv,0,u}}{2\sigma_1} \|\Delta v_h\|_{L^2(\Omega_i)}^2 + \frac{\beta}{2\varepsilon} \|[\mathbf{n}\cdot\nabla v_h]\|_{L^2(F)}^2 \right). \tag{4.48}$$

Then, using (4.47) and (4.48),

$$a_h(v_h, v_h) \geqslant \sum_{i=1}^{N} \|\Delta v_h\|_{L^2(\Omega_i)}^2 + \sum_{F\in\mathcal{F}} \frac{\sigma_0}{h_i^3}\|[v_h]\|_{L^2(F)}^2 + \sum_{F\in\mathcal{F}} \int_F \frac{\sigma_1}{h_i}\|[\mathbf{n}\cdot\nabla v_h]\|_{L^2(F)}^2$$

$$
\begin{aligned}
&- \varepsilon \frac{C_{inv,0,u}}{\sigma_1} \sum_{i=1}^{N} \|\Delta v_h\|^2_{L^2(\Omega_i)} - \frac{1}{\varepsilon} \sum_{F \in \mathcal{F}} \frac{\sigma_1}{h_i} \|[\mathbf{n} \cdot \nabla v_h]\|^2_{L^2(F)} \\
&- 2 \sum_{F \in \mathcal{F}} \left(\varepsilon \frac{C_{inv,0,1,u}}{2\sigma_0} \|\Delta v_h\|^2_{L^2(\Omega_i)} + \frac{\alpha}{2\varepsilon} \|[v_h]\|^2_{L^2(F)} \right) \\
&= \sum_{i=1}^{N} \|\Delta v_h\|^2_{L^2(\Omega_i)} + \sum_{F \in \mathcal{F}} \frac{\sigma_0}{h_i^3} \|[v_h]\|^2_{L^2(F)} + \sum_{F \in \mathcal{F}} \int_F \frac{\sigma_1}{h_i} \|[\mathbf{n} \cdot \nabla v_h]\|^2_{L^2(F)} \\
&- \varepsilon \frac{C_{inv,0,u}}{\sigma_1} \sum_{i=1}^{N} \|\Delta v_h\|^2_{L^2(\Omega_i)} - \frac{1}{\varepsilon} \sum_{F \in \mathcal{F}} \frac{\sigma_1}{h_i} \|[\mathbf{n} \cdot \nabla v_h]\|^2_{L^2(F)} \\
&- \varepsilon \frac{C_{inv,0,1,u}}{\sigma_0} \sum_{i=1}^{N} \|\Delta v_h\|^2_{L^2(\Omega_i)} - \frac{1}{\varepsilon} \sum_{F \in \mathcal{F}} \frac{\sigma_0}{h_i^3} \|[v_h]\|^2_{L^2(F)} \\
&= \left(1 - \varepsilon \frac{C_{inv,0,u}}{\sigma_1} - \varepsilon \frac{C_{inv,0,1,u}}{\sigma_0} \right) \sum_{i=1}^{N} \|\Delta v_h\|^2_{L^2(\Omega_i)} \\
&+ \left(1 - \frac{1}{\varepsilon} \right) \sum_{F \in \mathcal{F}} \frac{\sigma_0}{h_i^3} \|[v_h]\|^2_{L^2(F)} \\
&+ \left(1 - \frac{1}{\varepsilon} \right) \sum_{F \in \mathcal{F}} \frac{\sigma_1}{h_i} \|[\mathbf{n} \cdot \nabla v_h]\|^2_{L^2(F)} \\
&= \left(1 - \varepsilon \left(\frac{C_{inv,0,1,u}}{\sigma_0} + \frac{C_{inv,0,u}}{\sigma_1} \right) \right) \sum_{i=1}^{N} \|\Delta v_h\|^2_{L^2(\Omega_i)} \\
&+ \left(1 - \frac{1}{\varepsilon} \right) \sum_{F \in \mathcal{F}} \frac{\sigma_0}{h_i^3} \|[v_h]\|^2_{L^2(F)} \\
&+ \left(1 - \frac{1}{\varepsilon} \right) \sum_{F \in \mathcal{F}} \frac{\sigma_1}{h_i} \|[\mathbf{n} \cdot \nabla v_h]\|^2_{L^2(F)}. \qquad (4.49)
\end{aligned}
$$

The coefficients in (4.49) are required to be positive, that is

$$
1 - \frac{1}{\varepsilon} > 0, \quad \text{and} \quad 1 - \varepsilon \left(\frac{C_{inv,0,1,u}}{\sigma_0} + \frac{C_{inv,0,u}}{\sigma_1} \right) > 0.
$$

This implies that

$$
1 > \frac{1}{\varepsilon}, \quad \text{and} \quad 1 > \varepsilon \left(\frac{C_{inv,0,1,u}}{\sigma_0} + \frac{C_{inv,0,u}}{\sigma_1} \right).
$$

It follows that

$$\left(\frac{C_{inv,0,1,u}}{\sigma_0}+\frac{C_{inv,0,u}}{\sigma_1}\right)<\frac{1}{\varepsilon}<1.$$

Let ε and μ_c be chosen such that simultaneously,

$$0<\mu_c<1-\frac{1}{\varepsilon},\quad \text{and}\quad 0<\mu_c<1-\varepsilon\left(\frac{C_{inv,0,1,u}}{\sigma_0}+\frac{C_{inv,0,u}}{\sigma_1}\right).$$

It then follows that

$$a_h(v_h,v_h)\geqslant \mu_c\|v_h\|_h^2.$$

□

To prove for boundedness of the bilinear form $a_h(\cdot,\cdot):V_h^*\times V_h\longrightarrow\mathbb{R}$, where $V_h^*:=H^4(\Omega,\mathcal{T}_h)+V_h$. The following norm is defined on V_h^*

$$\|v\|_{V_h^*}=\left[\|v\|_h^2+\sum_{F\in\mathcal{F}}\frac{h_i^3}{\sigma_0}\|\{\mathbf{n}\cdot\nabla\Delta v\}\|_{L^2(F)}^2+\sum_{F\in\mathcal{F}}\frac{h_i}{\sigma_1}\|\{\Delta v\}\|_{L^2(F)}^2\right]^{\frac{1}{2}}. \tag{4.50}$$

Lemma 4.5.7. *Let $a_h(\cdot,\cdot):V_h^*\times V_h$ be the bilinear form defined in* (4.29)*, then there exists a positive constant μ_b, such that*

$$|a_h(u,v_h)|\leqslant\mu_b\|u\|_{V_h^*}\|v_h\|_h,\quad \forall u\in V_h^*,\ v_h\in V_h. \tag{4.51}$$

Proof. Using the triangle inequality,

$$\begin{aligned}|a_h(u,v_h)|=\Bigg|&\sum_{i=1}^N\int_{\Omega_i}\Delta u\Delta v_h\,\mathrm{d}\Omega\\&-\sum_{F\in\mathcal{F}}\int_F\{\Delta u\}[\mathbf{n}\cdot\nabla v_h]\,\mathrm{d}\Gamma-\sum_{F\in\mathcal{F}}\int_F[\mathbf{n}\cdot\nabla u]\{\Delta v_h\}\,\mathrm{d}\Gamma\\&+\sum_{F\in\mathcal{F}}\int_F\{\mathbf{n}\cdot\nabla\Delta u\}[v_h]\,\mathrm{d}\Gamma+\sum_{F\in\mathcal{F}}\int_F[u]\{\mathbf{n}\cdot\nabla\Delta v_h\}\,\mathrm{d}\Gamma\\&+\sum_{F\in\mathcal{F}}\frac{\sigma_0}{h_i^3}\int_F[u][v]\,\mathrm{d}\Gamma+\sum_{F\in\mathcal{F}}\frac{\sigma_1}{h_i}\int_F[\mathbf{n}\cdot\nabla u][\mathbf{n}\cdot\nabla v_h]\,\mathrm{d}\Gamma\Bigg|\end{aligned}$$

$$
\begin{aligned}
&\leqslant \left| \sum_{i=1}^{N} \int_{\Omega_i} \Delta u \Delta v_h \, \mathrm{d}\Omega \right| \\
&+ \left| \sum_{F \in \mathcal{F}} \int_F [\mathbf{n} \cdot \nabla u] \{\Delta v_h\} \, \mathrm{d}\Gamma \right| + \left| \sum_{F \in \mathcal{F}} \int_F \{\Delta u\} [\mathbf{n} \cdot \nabla v_h] \, \mathrm{d}\Gamma \right| \\
&+ \left| \sum_{F \in \mathcal{F}} \int_F \{\mathbf{n} \cdot \nabla \Delta u\} [v_h] \, \mathrm{d}\Gamma \right| + \left| \sum_{F \in \mathcal{F}} \int_F [u] \{\mathbf{n} \cdot \nabla \Delta v_h\} \, \mathrm{d}\Gamma \right| \\
&+ \left| \sum_{F \in \mathcal{F}} \frac{\sigma_0}{h_i^3} \int_F [u][v_h] \, \mathrm{d}\Gamma \right| + \left| \sum_{F \in \mathcal{F}} \frac{\sigma_1}{h_i} \int_F [\mathbf{n} \cdot \nabla u][\mathbf{n} \cdot \nabla v_h] \, \mathrm{d}\Gamma \right|.
\end{aligned}
$$

For the first term, using the Cauchy-Schwarz inequality gives

$$
\begin{aligned}
\left| \sum_{i=1}^{N} \int_{\Omega_i} \Delta u \Delta v_h \, \mathrm{d}\Omega \right| &\leqslant \left(\sum_{i=1}^{N} \int_{\Omega_i} |\Delta u|^2 \, \mathrm{d}\Omega \right)^{\frac{1}{2}} \left(\sum_{i=1}^{N} \int_{\Omega_i} |\Delta v_h|^2 \, \mathrm{d}\Omega \right)^{\frac{1}{2}} \\
&= \left(\sum_{i=1}^{N} \|\Delta u\|^2_{L^2(\Omega_i)} \right)^{\frac{1}{2}} \left(\sum_{i=1}^{N} \|\Delta v_h\|^2_{L^2(\Omega_i)} \right)^{\frac{1}{2}} \\
&\leqslant \|u\|_{V_h^*} \|v_h\|_h \, .
\end{aligned}
$$

For the second term, using the Cauchy-Schwarz inequality and the inverse inequalities,

$$
\begin{aligned}
&\left| \sum_{F \in \mathcal{F}} \int_F \frac{\sqrt{\sigma_1}}{\sqrt{h_i}} [\mathbf{n} \cdot \nabla u] \frac{\sqrt{h_i}}{\sqrt{\sigma_1}} \{\Delta v_h\} \, \mathrm{d}\Gamma \right| \\
&\leqslant \left(\sum_{F \in \mathcal{F}} \int_F \frac{\sigma_1}{h_i} |[\mathbf{n} \cdot \nabla u]|^2 \, \mathrm{d}\Gamma \right)^{\frac{1}{2}} \left(\sum_{F \in \mathcal{F}} \int_F \frac{h_i}{\sigma_1} |\{\Delta v_h\}|^2 \, \mathrm{d}\Gamma \right)^{\frac{1}{2}} \\
&\leqslant \|u\|_{V_h^*} \left(\frac{h_i}{\sigma_1} \sum_{F \in \mathcal{F}} \frac{1}{4} \|\Delta v_{h,i} + \Delta v_{h,j}\|^2_{L^2(F)} \right)^{\frac{1}{2}} \\
&\leqslant \|u\|_{V_h^*} \left(\frac{h_i}{2\sigma_1} \sum_{F \in \mathcal{F}} \left(\|\Delta v_{h,i}\|^2_{L^2(F)} + \|\Delta v_{h,j}\|^2_{L^2(F)} \right) \right)^{\frac{1}{2}}
\end{aligned}
$$

$$
\begin{aligned}
&= \|u\|_{V_h^*} \left(\frac{h_i}{2\sigma_1} \sum_{i=1}^{N} \|\Delta v_{h,i}\|^2_{L^2(\partial\Omega_i \setminus (\partial\Omega_i \bigcap \partial\Omega))} \right)^{\frac{1}{2}} \\
&\leqslant \|u\|_{V_h^*} \left(\frac{h_i}{2\sigma_1} \sum_{i=1}^{N} \|\Delta v_{h,i}\|^2_{L^2(\partial\Omega_i)} \right)^{\frac{1}{2}} \\
&\leqslant \|u\|_{V_h^*} \left(\frac{h_i}{2\sigma_1} C^2_{inv,0,u} \sum_{i=1}^{N} h_i^{-1} \|\Delta v_{h,i}\|^2_{L^2(\Omega_i)} \right)^{\frac{1}{2}} \\
&\leqslant \|u\|_{V_h^*} \frac{C_{inv,0,u}}{\sqrt{\sigma_1}} \left(\sum_{i=1}^{N} \|\Delta v_{h,i}\|^2_{L_2(\Omega_i)} \right)^{\frac{1}{2}} \\
&\leqslant \frac{C_{inv,0,u}}{\sqrt{\sigma_1}} \|u\|_{V_h^*} \|v_h\|_h,
\end{aligned}
$$

where $C_{inv,0,u}$ is the shape constant from the inverse inequalities.

For the third term, using the Cauchy-Schwarz inequality,

$$
\begin{aligned}
&\left| \sum_{F \in \mathcal{F}} \int_F \frac{\sqrt{h_i}}{\sqrt{\sigma_1}} \{\Delta u\} \frac{\sqrt{\sigma_1}}{\sqrt{h_i}} [\mathbf{n} \cdot \nabla v_h] \, \mathrm{d}\Gamma \right| \\
&\leqslant \left(\sum_{F \in \mathcal{F}} \int_F \frac{h_i}{\sigma_1} |\{\Delta u\}|^2 \, \mathrm{d}\Gamma \right)^{\frac{1}{2}} \left(\sum_{F \in \mathcal{F}} \int_F \frac{\sigma_1}{h_i} |[\mathbf{n} \cdot \nabla v_h]|^2 \, \mathrm{d}\Gamma \right)^{\frac{1}{2}} \\
&= \left(\sum_{F \in \mathcal{F}} \frac{h_i}{\sigma_1} \|\{\Delta u\}\|^2_{L^2(F)} \right)^{\frac{1}{2}} \left(\sum_{F \in \mathcal{F}} \frac{\sigma_1}{h_i} \|[\mathbf{n} \cdot \nabla v_h]\|^2_{L^2(F)} \right)^{\frac{1}{2}} \\
&\leqslant \|u\|_{V_h^*} \|v_h\|_h \, .
\end{aligned}
$$

For the fourth term, using the Cauchy-Schwarz inequality,

$$
\begin{aligned}
&\left| \sum_{F \in \mathcal{F}} \int_F \frac{h_i^{3/2}}{\sqrt{\sigma_0}} \{\mathbf{n} \cdot \nabla \Delta u\} \frac{\sqrt{\sigma_0}}{h_i^{3/2}} [\mathbf{n} \cdot \nabla v_h] \, \mathrm{d}\Gamma \right| \\
&\leqslant \left(\sum_{F \in \mathcal{F}} \int_F \frac{h_i^3}{\sigma_0} |\{\mathbf{n} \cdot \nabla \Delta u\}|^2 \, \mathrm{d}\Gamma \right)^{\frac{1}{2}} \left(\sum_{F \in \mathcal{F}} \int_F \frac{\sigma_0}{h_i^3} |[\mathbf{n} \cdot \nabla v_h]|^2 \, \mathrm{d}\Gamma \right)^{\frac{1}{2}}
\end{aligned}
$$

$$= \left(\sum_{F\in\mathcal{F}} \frac{h_i^3}{\sigma_0} \|\{\mathbf{n}\cdot\nabla\Delta u\}\|^2_{L^2(F)} \right)^{\frac{1}{2}} \left(\sum_{F\in\mathcal{F}} \frac{\sigma_0}{h_i^3} |[\mathbf{n}\cdot\nabla v_h]\|^2_{L^2(F)} \right)^{\frac{1}{2}}$$

$$\leqslant \|u\|_{V_h^*} \|v_h\|_h \,.$$

For the fifth term, using the Cauchy-Schwarz inequality, and following steps similar to those used for obtaining the bounds for the second term gives

$$\left| \sum_{F\in\mathcal{F}} \int_F \frac{\sqrt{\sigma_0}}{h_i^{3/2}} [\mathbf{n}\cdot\nabla u] \frac{h_i^{3/2}}{\sqrt{\sigma_0}} \{\mathbf{n}\cdot\nabla\Delta v_h\} \,\mathrm{d}\Gamma \right|$$

$$\leqslant \left(\sum_{F\in\mathcal{F}} \int_F \frac{\sigma_0}{h_i^3} |[\mathbf{n}\cdot\nabla u]|^2 \,\mathrm{d}\Gamma \right)^{\frac{1}{2}} \left(\sum_{F\in\mathcal{F}} \int_F \frac{h_i^3}{\sigma_0} |\{\mathbf{n}\cdot\nabla\Delta v_h\}|^2 \,\mathrm{d}\Gamma \right)^{\frac{1}{2}}$$

$$\leqslant \|u\|_{V_h^*} \left(\sum_{F\in\mathcal{F}} \frac{h_i^3}{\sigma_0} \frac{1}{4} \|\mathbf{n}\cdot\nabla\Delta v_{h,i} + \mathbf{n}\cdot\nabla\Delta v_{h,j}\|^2_{L^2(F)} \right)^{\frac{1}{2}}$$

$$\leqslant \|u\|_{V_h^*} \left(\frac{h_i^3}{\sigma_0} \sum_{F\in\mathcal{F}} \frac{1}{2} \big(\|\mathbf{n}\cdot\nabla\Delta v_{h,i}\|^2_{L^2(F)} + \|\mathbf{n}\cdot\nabla\Delta v_{h,j}\|^2_{L^2(F)} \big) \right)^{\frac{1}{2}}$$

$$= \|u\|_{V_h^*} \left(\frac{h_i^3}{2\sigma_0} \sum_{i=1}^{N} \|\nabla\Delta v_{h,i}\|^2_{L_2(\partial\Omega_i \setminus (\partial\Omega_i \bigcap \partial\Omega))} \right)^{\frac{1}{2}}$$

$$\leqslant \|u\|_{V_h^*} \left(\frac{h_i^3}{2\sigma_0} \sum_{i=1}^{N} \|\nabla\Delta v_{h,i}\|^2_{L_2(\partial\Omega_i)} \right)^{\frac{1}{2}}$$

$$\leqslant \|u\|_{V_h^*} \left(\frac{h_i^3}{2\sigma_0} C^2_{inv,0,1,u} \sum_{i=1}^{N} h_i^{-3} \|\Delta v_{h,i}\|^2_{L_2(\Omega_i)} \right)^{\frac{1}{2}}$$

$$\leqslant \|u\|_{V_h^*} \frac{C_{inv,0,1,u}}{\sqrt{\sigma_0}} \left(\sum_{i=1}^{N} \|\Delta v_{h,i}\|^2_{L_2(\Omega_i)} \right)^{\frac{1}{2}}$$

$$\leqslant \frac{C_{inv,0,1,u}}{\sqrt{\sigma_0}} \|u\|_{V_h^*} \|v_h\|_h \,.$$

For the sixth and seventh terms, using the Cauchy-Schwarz inequality,

$$\begin{aligned}\left|\sum_{F\in\mathcal{F}}\frac{\sigma_0}{h_i^3}\int_F[u][v]\,\mathrm{d}\Gamma\right| &\leqslant \left(\sum_{F\in\mathcal{F}}\int_F\frac{\sigma_0}{h_i^3}|[u]|^2\,\mathrm{d}\Gamma\right)^{\frac{1}{2}}\left(\sum_{F\in\mathcal{F}}\int_F\frac{\sigma_0}{h_i^3}|[v_h]|^2\,\mathrm{d}\Gamma\right)^{\frac{1}{2}}\\ &= \left(\sum_{F\in\mathcal{F}}\frac{\sigma_0}{h_i^3}\|[u]\|^2_{L_2(F)}\right)^{\frac{1}{2}}\left(\sum_{F\in\mathcal{F}}\frac{\sigma_0}{h_i^3}\|[v_h]\|^2_{L_2(F)}\right)^{\frac{1}{2}}\\ &\leqslant \|u\|_{V_h^*}\|v_h\|_h,\end{aligned}$$

and

$$\begin{aligned}&\left|\sum_{F\in\mathcal{F}}\frac{\sigma_1}{h_i}\int_F[\mathbf{n}\cdot\nabla u][\mathbf{n}\cdot\nabla v_h]\,\mathrm{d}\Gamma\right|\\ &\leqslant \left(\sum_{F\in\mathcal{F}}\int_F\frac{\sigma_1}{h_i}|[\mathbf{n}\cdot\nabla u]|^2\,\mathrm{d}\Gamma\right)^{\frac{1}{2}}\left(\sum_{F\in\mathcal{F}}\int_F\frac{\sigma_1}{h_i}|[\mathbf{n}\cdot\nabla v_h]|^2\,\mathrm{d}\Gamma\right)^{\frac{1}{2}}\\ &= \left(\sum_{F\in\mathcal{F}}\frac{\sigma_1}{h_i}\|[\mathbf{n}\cdot\nabla u]\|^2_{L_2(F)}\right)^{\frac{1}{2}}\left(\sum_{F\in\mathcal{F}}\frac{\sigma_1}{h_i}\|[\mathbf{n}\cdot\nabla v_h]\|^2_{L_2(F)}\right)^{\frac{1}{2}}\\ &\leqslant \|u\|_{V_h^*}\|v_h\|_h\,.\end{aligned}$$

Then, summing all the bounds give

$$\begin{aligned}|a_h(u,v_h)| &\leqslant \|u\|_{V_h^*}\|v_h\|_h + \frac{C_{inv,0,u}}{\sqrt{\sigma_1}}\|u\|_{V_h^*}\|v_h\|_h + \|u\|_{V_h^*}\|v_h\|_h\\ &\quad + \|u\|_{V_h^*}\|v_h\|_h + \frac{C_{inv,0,1,u}}{\sqrt{\sigma_0}}\|u\|_{V_h^*}\|v_h\|_h + \|u\|_{V_h^*}\|v_h\|_h + \|u\|_{V_h^*}\|v_h\|_h\\ &= (5 + \frac{C_{inv,0,u}}{\sqrt{\sigma_1}} + \frac{C_{inv,0,1,u}}{\sqrt{\sigma_0}})\|u\|_{V_h^*}\|v_h\|_h\,.\end{aligned}$$

Thus $|a_h(u,v_h)| \leqslant \mu_b\|u\|_{V_h^*}\|v_h\|_h$, with $\mu_b = 5 + \frac{C_{inv,0,u}}{\sqrt{\sigma_1}} + \frac{C_{inv,0,1,u}}{\sqrt{\sigma_0}}$. □

4.6 Approximation and Error Estimates

In this section, the discretization error estimates of the symmetric interior penalty scheme are presented and an *a-priori* error estimate is derived. Some auxiliary results

are required to analyze the dG-IgA scheme.

4.6.1 Auxiliary Results

Theorem 4.6.1. *Let l and s be non-zero integers with $0 \leqslant l \leqslant s \leqslant p+1$ and $\widehat{K} \in \widehat{\mathcal{K}}_h$ such that $K = \Phi(\widehat{K})$. Then there exists an interpolant $\Pi_h v \in V_h$ for all $v \in L^2(\Omega) \bigcap H^s(\bar{K})$ and a constant $C_s > 0$ such that the following inequality holds*

$$|v - \Pi_h v|_{H^l(K)} \leqslant C_s h_K^{s-l} \sum_{t=0}^{s} \|\nabla \Phi\|^{t-s}_{L^\infty(\overline{\widehat{K}})} \|v\|_{H^t(\bar{K})}, \tag{4.52}$$

where h_K is the element size in the physical domain defined as $h_K = \|\nabla \Phi\|_{L^\infty(\widehat{K})} \widehat{h}_{\widehat{K}}$.

Proof. See [Theorem 3.1 in Bazilevs et al. (2006)]. □

Proposition 4.6.2. *Given the integers l and s such that $0 \leqslant l \leqslant s \leqslant p+1$, there exist a positive constant C_s such that for a function $v \in H^s(\Omega_i)$*

$$\sum_{K \in \mathcal{K}_{h,i}} |v - \Pi_{h,i} v|^2_{H^l(K)} \leqslant C_s h^{2(s-l)} \|v\|^2_{H^s(\Omega_i)}, \tag{4.53}$$

where h_i is the mesh size in the physical domain, and p denotes the underlying B-spline or NURBS degree.

Proof. See [Proposition 3.1 in Tagliabue et al. (2014)]. □

Proposition 4.6.3. *Given the integers l and s such that $0 \leqslant l \leqslant s \leqslant p+1$, there exist a positive constant C_s such that for a function $v \in H^s(\Omega_i)$ and $l \leqslant k_{min}$; k_{min} being the global smoothness parameter for the NURBS basis*

$$|v - \Pi_{h,i} v|_{H^l(\Omega_i)} \leqslant C_s h_i^{(s-l)} \|v\|_{H^s(\Omega_i)}, \tag{4.54}$$

where h_i denotes the maximum mesh-size parameter in the physical domain, Ω_i.

Proof. See [Proposition 3.2 in Tagliabue et al. (2014)]. □

Lemma 4.6.4. *Let s and p be positive integers such that $s \geqslant 4$ and $p \geqslant 3$. Then there exists an interpolant, $\Pi_{h,i} : H^s(\Omega, \mathcal{T}_h) \longrightarrow V_h$, $\Pi_{h,i} v \in V_h$ for all $v \in H^s(\Omega, \mathcal{T}_h)$ with $C_0, C_1, C_2, C_3, C_4 > 0$ such that for $F \in \mathcal{F}$ the following estimates hold*

$$\|\nabla^q (v - \Pi_{h,i} v)\|^2_{L^2(\partial\Omega_i)} \leqslant C_0 h_i^{2(r_i - q) - 1} \|v\|^2_{H^{r_i}(\Omega_i)}, \tag{4.55}$$

$$\sum_{F \in \mathcal{F}} \frac{\sigma_0}{h_i^3} \|[v - \Pi_{h,i} v]\|^2_{L^2(F)} \leqslant C_1 \sum_{i=1}^{N} h_i^{2(r_i - 2)} \|v\|^2_{H^{r_i}(\Omega_i)}, \tag{4.56}$$

$$\sum_{F \in \mathcal{F}} \frac{\sigma_1}{h_i} \|[\mathbf{n} \cdot \nabla (v - \Pi_{h,i} v)]\|^2_{L^2(F)} \leqslant C_2 \sum_{i=1}^{N} h_i^{2(r_i - 2)} \|v\|^2_{H^{r_i}(\Omega_i)}, \tag{4.57}$$

$$\sum_{F \in \mathcal{F}} \frac{h_i}{\sigma_1} \|\{\Delta (v - \Pi_{h,i} v)\}\|^2_{L^2(F)} \leqslant C_3 \sum_{i=1}^{N} h_i^{2(r_i - 2)} \|v\|^2_{H^{r_i}(\Omega_i)}, \tag{4.58}$$

$$\sum_{F \in \mathcal{F}} \frac{h_i^3}{\sigma_0} \|\{\mathbf{n} \cdot \nabla \Delta (v - \Pi_{h,i} v)\}\|^2_{L^2(F)} \leqslant C_4 \sum_{i=1}^{N} h_i^{2(r_i - 2)} \|v\|^2_{H^{r_i}(\Omega_i)}, \tag{4.59}$$

where $q \geqslant 0, r_i = \min\{s, p+1\}$ and C_0, C_1, C_2, C_3 and C_4 are independent of the mesh size but factors of the penalty parameters σ_0 and σ_1.

Proof. For (4.55), using Lemma 4.5.2, and the approximation estimate in Proposition 4.6.3,

$$\begin{aligned}
\|\nabla^q (v - \Pi_{h,i} v)\|^2_{L^2(\partial\Omega_i)} &\leqslant C^2_{tr,u} h_i^{-1} \left(\|\nabla^q (v - \Pi_{h,i} v)\|^2_{L^2(\Omega_i)} + h_i^2 |\nabla^q (v - \Pi_{h,i} v)|^2_{H^1(\Omega_i)} \right) \\
&= C^2_{tr,u} h_i^{-1} \left(|v - \Pi_{h,i} v|^2_{H^q(\Omega_i)} + h_i^2 |v - \Pi_{h,i} v|^2_{H^{q+1}(\Omega_i)} \right) \\
&\leqslant C_s^2 C^2_{tr,u} h_i^{-1} \left(h_i^{2(r_i - q)} \|v\|^2_{H^{r_i}(\Omega_i)} + h_i^2 h_i^{2(r_i - q - 1)} \|v\|^2_{H^{r_i}(\Omega_i)} \right) \\
&= C_s^2 C^2_{tr,u} h_i^{-1} \left(h_i^{2(r_i - q)} + h_i^{2(r_i - q)} \right) \|v\|^2_{H^{r_i}(\Omega_i)} \\
&\leqslant C_0 h_i^{-1} h_i^{2(r_i - q)} \|v\|^2_{H^{r_i}(\Omega_i)} = C_0 h_i^{2(r_i - q) - 1} \|v\|^2_{H^{r_i}(\Omega_i)},
\end{aligned}$$

with $C_0 = 2 C_s^2 C^2_{tr,u}$.

For (4.56), setting $q = 0$ in (4.55),

$$\sum_{F \in \mathcal{F}} \frac{\sigma_0}{h_i^3} \|[v - \Pi_{h,i} v]\|^2_{L^2(F)} = \sum_{F \in \mathcal{F}} \frac{\sigma_0}{h_i^3} \|(v - \Pi_{h,i} v) - (v - \Pi_{h,j} v)\|^2_{L^2(F)}$$

$$
\begin{aligned}
&\leqslant \sum_{F\in\mathcal{F}} 2\frac{\sigma_0}{h_i^3}\Big(\|v-\Pi_{h,i}v\|^2_{L^2(F)}+\|v-\Pi_{h,j}v\|^2_{L^2(F)}\Big)\\
&=\sum_{i=1}^{N} 2\frac{\sigma_0}{h_i^3}\|v-\Pi_{h,i}v\|^2_{L^2(\partial\Omega_i\setminus(\partial\Omega_i\bigcap\partial\Omega))}\\
&\leqslant \sum_{i=1}^{N} 2\frac{\sigma_0}{h_i^3}\|v-\Pi_{h,i}v\|^2_{L^2(\partial\Omega_i)}\\
&\leqslant \sum_{i=1}^{N} 2\frac{\sigma_0}{h_i^3}C_0h_i^{2r_i-1}\|v\|^2_{H^{r_i}(\Omega_i)}=C_1\sum_{i=1}^{N}h_i^{2(r_i-2)}\|v\|^2_{H^{r_i}(\Omega_i)},
\end{aligned}
\tag{4.60}
$$

with $C_1=2\sigma_0C_0$.

For (4.57), setting $q=1$ in (4.55),

$$
\begin{aligned}
&\sum_{F\in\mathcal{F}}\frac{\sigma_1}{h_i}\|[\mathbf{n}\cdot\nabla(v-\Pi_{h,i}v)]\|^2_{L^2(F)}\\
&=\sum_{F\in\mathcal{F}}\frac{\sigma_1}{h_i}\|\mathbf{n}\cdot\nabla(v-\Pi_{h,i}v)-\mathbf{n}\cdot\nabla(v-\Pi_{h,j}v)\|^2_{L^2(F)}\\
&\leqslant\sum_{F\in\mathcal{F}}2\frac{\sigma_1}{h_i}\Big(\|\nabla(v-\Pi_{h,i}v)\|^2_{L^2(F)}+\|\nabla(v-\Pi_{h,j}v)\|^2_{L^2(F)}\Big)\\
&=\sum_{i=1}^{N}2\frac{\sigma_1}{h_i}\|\nabla(v-\Pi_{h,i}v)\|^2_{L^2(\partial\Omega_i\setminus(\partial\Omega_i\bigcap\partial\Omega))}\\
&\leqslant\sum_{i=1}^{N}2\frac{\sigma_1}{h_i}\|\nabla(v-\Pi_{h,i}v)\|^2_{L^2(\partial\Omega_i)}\\
&\leqslant\sum_{i=1}^{N}2\frac{\sigma_1}{h_i}C_0h_i^{2(r_i-1)-1}\|v\|^2_{H^{r_i}(\Omega_i)}=C_2\sum_{i=1}^{N}h_i^{2(r_i-2)}\|v\|^2_{H^{r_i}(\Omega_i)},
\end{aligned}
\tag{4.61}
$$

with $C_2=2\sigma_1C_0$.

For (4.58), setting $q=2$ in (4.55),

$$
\sum_{F\in\mathcal{F}}\frac{h_i}{\sigma_1}\|\{\Delta(v-\Pi_{h,i}v)\}\|^2_{L^2(F)}
$$

$$= \sum_{F\in\mathcal{F}} \frac{h_i}{4\sigma_1}\|\Delta(v-\Pi_{h,i}v)+\Delta(v-\Pi_{h,j}v)\|^2_{L^2(F)}$$

$$\leqslant \sum_{F\in\mathcal{F}} 2\frac{h_i}{4\sigma_1}\left(\|\Delta(v-\Pi_{h,i}v)\|^2_{L^2(F)}+\|\Delta(v-\Pi_{h,j}v)\|^2_{L^2(F)}\right)$$

$$= \sum_{i=1}^{N} \frac{h_i}{2\sigma_1}\|\Delta(v-\Pi_{h,i}v)\|^2_{L^2(\partial\Omega_i\setminus(\partial\Omega_i\bigcap\partial\Omega))}$$

$$\leqslant \sum_{i=1}^{N} \frac{h_i}{2\sigma_1}\|\Delta(v-\Pi_{h,i}v)\|^2_{L^2(\partial\Omega_i)}$$

$$\leqslant \sum_{i=1}^{N} \frac{h_i}{2\sigma_1}C_0 h_i^{2(r_i-2)-1}\|v\|^2_{H^{r_i}(\Omega_i)} = C_3\sum_{i=1}^{N} h_i^{2(r_i-2)}\|v\|^2_{H^{r_i}(\Omega_i)},$$

with $C_3 = \frac{C_0}{2\sigma_1}$.

For (4.59), setting $q = 3$ in 4.55,

$$\sum_{F\in\mathcal{F}} \frac{h_i^3}{\sigma_0}\|\{\mathbf{n}\cdot\nabla\Delta(v-\Pi_{h,i}v)\}\|^2_{L^2(F)}$$

$$= \sum_{F\in\mathcal{F}} \frac{h_i^3}{4\sigma_0}\|\mathbf{n}\cdot\nabla\Delta(v-\Pi_{h,i}v)+\mathbf{n}\cdot\nabla\Delta(v-\Pi_{h,j}v)\|^2_{L^2(F)}$$

$$\leqslant \sum_{F\in\mathcal{F}} 2\frac{h_i^3}{4\sigma_0}\left(\|\nabla\Delta(v-\Pi_{h,i}v)\|^2_{L^2(F)}+\|\nabla\Delta(v-\Pi_{h,j}v)\|^2_{L^2(F)}\right)$$

$$= \sum_{i=1}^{N} \frac{h_i^3}{2\sigma_0}\|\nabla\Delta(v-\Pi_{h,i}v)\|^2_{L^2(\partial\Omega_i\setminus(\partial\Omega_i\bigcap\partial\Omega))}$$

$$\leqslant \sum_{i=1}^{N} \frac{h_i^3}{2\sigma_0}\|\nabla\Delta(v-\Pi_{h,i}v)\|^2_{L^2(\partial\Omega_i)}$$

$$\leqslant \sum_{i=1}^{N} \frac{h_i^3}{2\sigma_0}C_0 h_i^{2(r_i-3)-1}\|v\|^2_{H^{r_i}(\Omega_i)} = C_4\sum_{i=1}^{N} h_i^{2(r_i-2)}\|v\|^2_{H^{r_i}(\Omega_i)}. \tag{4.62}$$

with $C_4 = \frac{C_0}{2\sigma_0}$.

□

4.6.2 Error Estimates

To derive a priori error estimates, the following estimates are required.

Lemma 4.6.5. *Let $v \in H^s(\Omega, \mathcal{T}_h)$ for $s \geqslant 4$ be the solution of 4.29 and $\Pi_{h,i} v \in V_h$ be the continuous interpolant of v. Then, for $p \geqslant 3$, the following hold*

$$\|v - \Pi_{h,i} v\|_h^2 \leqslant C_5 \sum_{i=1}^{N} h_i^{2(r_i-2)} \|v\|_{H^{r_i}(\Omega_i)}^2, \tag{4.63}$$

$$\|v - \Pi_{h,i} v\|_{V_h^*}^2 \leqslant C_6 \sum_{i=1}^{N} h_i^{2(r_i-2)} \|v\|_{H^{r_i}(\Omega_i)}^2, \tag{4.64}$$

where $r_i := \min\{s, p+1\}$, C_5 and C_6 are independent of mesh sizes h_i.

Proof. By using the definition of the norm 4.32 and Lemma 4.6.4,

$$\begin{aligned}
&\|v - \Pi_{h,i} v\|_h^2 \\
&= \sum_{i=1}^{N} \|\Delta(v - \Pi_{h,i} v)\|_{L^2(\Omega_i)}^2 + \sum_{F \in \mathcal{F}} \frac{\sigma_0}{h_i^3} \|[v - \Pi_{h,i} v]\|_{L^2(F)}^2 \\
&+ \sum_{F \in \mathcal{F}} \frac{\sigma_1}{h_i} \|[\mathbf{n} \cdot \nabla(v - \Pi_{h,i} v)]\|_{L^2(F)}^2 \\
&\leqslant C_s \sum_{i=1}^{N} h_i^{2(r_i-2)} \|v\|_{H^{r_i}(\Omega_i)}^2 + C_1 \sum_{i=1}^{N} h_i^{2(r_i-2)} \|v\|_{H^{r_i}(\Omega_i)}^2 + C_2 \sum_{i=1}^{N} h_i^{2(r_i-2)} \|v\|_{H^{r_i}(\Omega_i)}^2 \\
&= C_5 \sum_{i=1}^{N} h_i^{2(r_i-2)} \|v\|_{H^{r_i}(\Omega_i)}^2,
\end{aligned}$$

where $C_5 = (C_s + C_1 + C_2)$.

Next, by using the definition of the norm 4.50 together with Lemma 4.6.4,

$$\begin{aligned}
\|v - \Pi_{h,i} v\|_{V_h^*}^2 = \|v - \Pi_{h,i} v\|_h^2 &+ \sum_{F \in \mathcal{F}} \frac{h_i^3}{\sigma_0} \|\{\mathbf{n} \cdot \nabla \Delta(v - \Pi_{h,i} v)\}\|_{L^2(F)}^2 \\
&+ \sum_{F \in \mathcal{F}} \frac{h_i}{\sigma_1} \|\{\Delta(v - \Pi_{h,i} v)\}\|_{L^2(F)}^2
\end{aligned}$$

$$\leqslant C_5 \sum_{i=1}^{N} h_i^{2(r_i-2)} \|v\|^2_{H^{r_i}(\Omega_i)} + C_3 \sum_{i=1}^{N} h_i^{2(r_i-2)} \|v\|^2_{H^{r_i}(\Omega_i)}$$

$$+ C_4 \sum_{i=1}^{N} h_i^{2(r_i-2)} \|v\|^2_{H^{r_i}(\Omega_i)}$$

$$= C_6 \sum_{i=1}^{N} h_i^{2(r_i-2)} \|v\|^2_{H^{r_i}(\Omega_i)},$$

where $C_6 = (C_5 + C_3 + C_4)$. □

Finally, the *a-priori* discretization error estimate in the discrete norm $\|\cdot\|_h$ is stated in the following theorem.

Theorem 4.6.6. *Let $u \in H^s(\Omega, \mathcal{T}_h)$ with $s \geqslant 4$, be the solution of 4.26, and let $u_h \in V_h$ be the solution of 4.29. Then there exists $C > 0$, independent of h_i and N such that the following bound holds*

$$\|u - u_h\|_h \leqslant C \sum_{i=1}^{N} h_i^{r_i-2} \|u\|_{H^{r_i}(\Omega_i)}, \tag{4.65}$$

where $r_i = \min\{s, p+1\}$ and C is independent of the mesh sizes h_i but dependent on the NURBS degree p.

Proof. By using the triangle inequality,

$$\|u - u_h\|_h \leqslant \|u - \Pi_{h,i} u\|_h + \|\Pi_{h,i} u - u_h\|_h \,. \tag{4.66}$$

By using the coercivity result, Galerkin orthogonality and the boundedness result,

$$\mu_c \|\Pi_{h,i} u - u_h\|_h^2 \leqslant a_h(\Pi_{h,i} u - u_h, \Pi_{h,i} u - u_h) = a_h(\Pi_{h,i} u - u, \Pi_{h,i} u - u_h)$$

$$\leqslant \mu_b \|\Pi_{h,i} u - u\|_{V_h^*} \|\Pi_{h,i} u - u_h\|_h.$$

Subsequently

$$\|\Pi_{h,i} u - u_h\|_h \leqslant \frac{\mu_b}{\mu_c} \|\Pi_{h,i} u - u\|_{V_h^*}.$$

Then

$$\begin{aligned}\|u-u_h\|_h &\leqslant \|u-\Pi_{h,i}u\|_h + \frac{\mu_b}{\mu_c}\|\Pi_{h,i}u-u\|_{V_h^*},\\ &\leqslant C_5^{1/2}\sum_{i=1}^{N} h_i^{r_i-2}\|u\|_{H^{r_i}(\Omega_i)} + \frac{\mu_b}{\mu_c}C_6^{1/2}\sum_{i=1}^{N} h_i^{r_i-2}\|u\|_{H^{r_i}(\Omega_i)}\\ &= C_7\sum_{i=1}^{N} h_i^{r_i-2}\|u\|_{H^{r_i}(\Omega_i)}, \end{aligned} \tag{4.67}$$

with $C_7 = C_5^{1/2} + \frac{\mu_b}{\mu_c}C_6^{1/2}$. □

Remark 4.6.1. *In the analysis performed in this chapter, it was assumed that s was the same for each $H^s(\Omega_i)$. In a more general case, the vector $\mathbf{s} = (s_1, \ldots, s_N)$ is defined such that $H^{\mathbf{s}}(\Omega, \mathcal{T}_h) := \{v \in L^2(\Omega) : v|_{\Omega_i} \in H^{s_i}(\Omega_i), \quad \forall i = 1, \ldots, N\}$. Also, for very complex geometry, the NURBS degree may vary significantly between patches, that is, it may be the case that $\mathbf{p} = (p_1, \ldots, p_N)$, with p_i not necessarily greater than 3.*

Chapter 5

Conclusion and Recommendations

5.1 Introduction

In this chapter, conclusions and recommendations for further studies are presented.

5.2 Conclusion

In this thesis, the standard Galerkin IgA approximation for the general biharmonic problem was derived, and the existence and uniqueness of the solution to the model problem was shown. The corresponding *a-priori* error estimates were also presented.

An interior penalty variational formulation of the Dirichlet version of the biharmonic problem was derived, and using the SIPG method, a dG-IgA scheme for the biharmonic problem was obtained. The variational formulation was shown to be consistent with the strong form of the problem.

Discrete coercivity and boundedness proofs for the bilinear form of the dG-IgA approximation, which guarantee the existence, uniqueness and stability of the solution

to the model problem were presented.

Some approximation estimates were obtained, and *a-priori* error estimates were presented for the dG-IgA scheme obtained. From the *a-priori* error estimates, numerical results are expected to converge optimally in the dG-norm, as is consistent with observed literature.

5.3 Recommendations

The following are recommended:

1. In the derivation of the dG-IgA schemes and for the numerical analysis carried out, the SIPG method, which is part of the class of primal discontinuous Galerkin methods was considered. There are three other methods in this class that can also be considered.

2. The a-priori error estimates presented in this thesis correspond to convergence analysis under h-refinement. Convergence can also be studied with respect to p-refinement and k-refinement.

REFERENCES

Adams, R. A. and Fournier, J. J. F. (2003), *Sobolev Spaces*, Volume 140 of Pure and Applied Mathematics: Academic Press, Amsterdam, Boston, second edn.

Arnold, D. N., Brezzi, F., Cockburn, B., and Marini, L. D. (2002), "Unified analysis of discontinuous Galerkin methods for elliptic problems," *SIAM Journal on Numerical Analysis*, 39, 1749–1779.

Auricchio, F., Beirão da Veiga, L., Buffa, A., Lovadina, C., Reali, A., and Sangalli, G. (2007), "A fully "locking-free" isogeometric approach for plane linear elasticity problems: a stream function formulation." *Comput Methods Appl Mech Engrg*, 197, 160–172.

Auricchio, F., Beirão da Veiga, L., Hughes, T. J. R., Reali, A., and Sangalli, G. (2010), "Isogeometric Collocaton Methods," *Mathematical Models and Methods in Applied Sciences*, 20, 2075–2107.

Bartezzaghi, A., Dedé, L., and Quarteroni, A. (2015), "IsogeometricAnalysis of high order Partial Differential Equations on surfaces," *Computer Methods in Applied Mechanics and Engineering*.

Bazilevs, Y., Beirão da Veiga, L., Cottrell, J. A., Hughes, T. J. R., and Sangalli, G. (2006), "Isogeometric Analysis: Approximation, stability and error estimates for h-refined meshes," *Mathematical Models and Methods in Applied Sciences*, 16, 1031–1090.

Beer, G. (2015), *Advanced Numerical Simulation Methods: From CAD Data Directly to Simulation Results*, CRC Press, Taylor & Francis Group.

Brenner, S. C. and Scott, L. R. (2008), *The Mathematical Theory of Finite Element Methods*, vol. 15 of *Texts in Applied Mathematics*, Springer Science+Business Media, third edn.

Brunero, F. (2012), "Discontinuous Galerkin Methods for Isogeometric Analysis," Master's thesis, Universitá degli Studi di Milano.

Ciarlet, P. G. (2002), *The Finite Element Method for Elliptic Problems*, SIAM: Classics in Applied Mathematics.

Cottrell, J. A., Reali, A., Bazilevs, Y., and Hughes, T. J. R. (2006), "Isogeometric analysis of structural vibrations," *Computer Methods in Applied Mechanics and Engineering*, 195, 5257–5296.

Cottrell, J. A., Hughes, T. J. R., and Bazilevs., Y. (2009), *Isogeometric Analysis: Toward Integration of CAD and FEA*, John Wiley & Sons, Ltd.

Engel, G., Garikipati, K., Hughes, T. J. R., Larson, M. G., Mazzei, L., and Taylor, R. L. (2002), "Continuous/discontinuous finite element approximations of fourth-order elliptic problems in structural and continuum mechanics with applications to thin beams and plates, and strain gradient elasticity." *Computer Methods in Applied Mechanics and Engineering*, 191, 3669–3750.

Gomez, H., Calo, V. M., and Hughes, T. J. R. (2009), *ECCOMAS Multidisciplinary Jubilee Symposium: New Computational Challenges in Materials, Structures, and Fluids*, chap. Isogeometric Analysis of Phase-Field Models: Application to the Cahn-Hilliard Equation, pp. 1–16, Springer Netherlands.

Hughes, T. J. R. (2000), *The Finite Element Method : Linear Static and Dynamic Finite Element Analysis*, Dover Publications, Inc.

Hughes, T. J. R., Cottrell, J. A., and Bazilevs, Y. (2005), "Isogeometric analysis: CAD, finite elements, NURBS, exact geometry and mesh refinement," *Comput. Methods Appl. Mech. Engrg*, 194, 4135–4195.

Hughes, T. J. R., Reali, A., and Sangalli, G. (2010), "Efficient Quadrature for NURBS-based Isogeometric Analysis," *Computer Methods in Applied Mechanics and Engineering*, 199, 301–313.

Jüttler, B., Langer, U., Mantzaflaris, A., Moore, S. E., and Zulehner, W. (2014), "Geometry + Simulation Modules: Implementing Isogeometric Analysis," *PAMM: Proc. Appl. Math. Mech.*, 14, 961–962.

Langer, U. and Moore, S. E. (2016), "Discontinuous Galerkin Isogeometric Analysis of Elliptic PDEs on Surfaces," *Lecture Notes in Computational Science and Engineering*, 104, 319–326.

Langer, U. and Toulopoulos, I. (2014), "Analysis of multipatch discontinuous Galerkin IgA approximations to elliptic boundary value problems," *Computing and Visualization in Science*, 17, 217–233.

Langer, U., Mantzaflaris, A., Moore, S. E., and Toulopoulos, I. (2014), "Multipatch Discontinuous Galerkin Isogeometric Analysis," *Lecture Notes in Computational Science and Engineering*, 107, 1–32.

Lions, J. L. and Magenes, E. (1972), *Non-Homogeneous Boudary Value Problems and Applications*, vol. I, Springer-Verlag Berlin Heidelberg.

Moore, S. E. (2017), "Nonstandard Discretization Strategies In Isogeometric Analysis for Partial Differential Equations." Ph.D. thesis, Johannes Kepler University.

Mozolevski, I. and Süli, E. (2003), "A Priori Error Analysis for the hp-Version of the Discontinuous Galerkin Finite Element Method for the Biharmonic Equation," *Computational Methods in Applied Mathematics*, 3, 596607.

Nečas, J. (2012), *Direct Methods in the Theory of Elliptic Equations*, Springer Monographs in Mathematics, Springer-Verlag Berlin Heidelberg.

Nguyen, V. P., Kerfriden, P., Brino, M., Bordas, S. P. A., and Bonisoli, E. (2014), "Nitsches method for two and three dimensional NURBS patch coupling," *Computational Mechanics*, 53, 11631182, Cite this article as: Nguyen, V. P., Kerfriden, P., Brino, M. et al.

Nguyen, V. P., Anitescu, C., Bordasa, S. P. A., and Rabczuk, T. (2015), "Isogeometric analysis: An overview and computer implementation aspects," *Mathematics and Computers in Simulation*, 117, 89–116.

Piegl, L. and Tiller, W. (1997), *The NURBS Book*, Monographs in Visual Communication, Springer-Verlag Berlin Heidelberg, second edn.

Pietro, D. A. D. and Ern, A. (2012), *Mathematical Aspects of Discontinuous Galerkin Methods*, Springer-Verlag Berlin Heidelberg.

Riviére, B. (2008), *Discontinuous Galerkin Methods for Solving Elliptic and Parabolic Equations: Theory and Implementation*, SIAM: Frontiers in Applied Mathematics.

Süli, E. and Mozolevski, I. (2007), "hp-version interior penalty DGFEMs for the biharmonic equation," *Computer Methods in Applied Mechanics and Engineering*, 196, 1851–1863.

Tagliabue, A., Dedé, L., and Quarteroni, A. (2014), "Isogeometric Analysis and error estimates for high order partial differential equations in fluid dynamics," *Computers & Fluids*, 102.

Vázquez, R. (2016), "A new design for the implementation of isogeometric analysis in Octave and Matlab: GeoPDEs 3.0," Tech. rep., Istituto di Matematica Applicata e Tecnologie Informatiche Enrico Magenes, IMATI REPORT Series.

Vuong, A. V., Heinrich, C., and Simeon, B. (2010), "ISOGAT: A 2D tutorial MATLAB code for Isogeometric Analysis," *Elsevier: Computer Aided Geometric Design*, 27, 644655.

Zhang, F., Xu, Y., and Chen, F. (2015), "Discontinuous Galerkin Methods for Isogeometric Analysis for Elliptic Equations on Surfaces," *Commun. Math. Stat.*, 2, 431–461.